Dysfunction in the βII Spectrin–Dependent Cytoskeleton Underlies Human Arrhythmia

Sakima A. Smith, MD; Amy C. Sturm, MS, CGC; Jerry Curran, PhD; Crystal F. Kline, PhD; Sean C. Little, PhD; Ingrid M. Bonilla, PhD; Victor P. Long, PharmD; Michael Makara, BS; Iuliia Polina, PhD; Langston D. Hughes; Tyler R. Webb; Zhiyi Wei, PhD; Patrick Wright, BS; Niels Voigt, MD; Deepak Bhakta, PhD; Katherine G. Spoonamore, PhD; Chuansheng Zhang, PhD; Raul Weiss, MD; Philip F. Binkley, MD; Paul M. Janssen, PhD; Ahmet Kilic, MD; Robert S. Higgins, MD; Mingzhai Sun, PhD; Jianjie Ma, PhD; Dobromir Dobrev, MD; Mingjie Zhang, PhD; Cynthia A. Carnes, PharmD, PhD; Matteo Vatta, MD; Matthew N. Rasband, PhD; Thomas J. Hund, PhD; Peter J. Mohler, PhD

Background—The cardiac cytoskeleton plays key roles in maintaining myocyte structural integrity in health and disease. In fact, human mutations in cardiac cytoskeletal elements are tightly linked to cardiac pathologies, including myopathies, aortopathies, and dystrophies. Conversely, the link between cytoskeletal protein dysfunction and cardiac electric activity is not well understood and often overlooked in the cardiac arrhythmia field.

Methods and Results—Here, we uncover a new mechanism for the regulation of cardiac membrane excitability. We report that βII spectrin, an actin-associated molecule, is essential for the posttranslational targeting and localization of critical membrane proteins in heart. βII spectrin recruits ankyrin-B to the cardiac dyad, and a novel human mutation in the ankyrin-B gene disrupts the ankyrin-B/βII spectrin interaction, leading to severe human arrhythmia phenotypes. Mice lacking cardiac βII spectrin display lethal arrhythmias, aberrant electric and calcium handling phenotypes, and abnormal expression/localization of cardiac membrane proteins. Mechanistically, βII spectrin regulates the localization of cytoskeletal and plasma membrane/sarcoplasmic reticulum protein complexes, including the Na/Ca exchanger, ryanodine receptor 2, ankyrin-B, actin, and αII spectrin. Finally, we observe accelerated heart failure phenotypes in βII spectrin–deficient mice.

Conclusions—Our findings identify βII spectrin as critical for normal myocyte electric activity, link this molecule to human disease, and provide new insight into the mechanisms underlying cardiac myocyte biology. (***Circulation*. 2015;131:695-708. DOI: 10.1161/CIRCULATIONAHA.114.013708.**)

Key Words: arrhythmias, cardiac ■ catecholaminergic polymorphic ventricular arrhythmia ■ cytoskeleton ■ ion channels ■ protein transport ■ ventricular tachycardia

Life for the vertebrate requires sustained and rhythmic beating of the heart for delivery of oxygen and nutrients to the brain and other organs. The vertebrate cardiomyocyte has evolved elegant membrane regulatory pathways to maintain efficient excitation-contraction coupling at baseline or in the face of acute and chronic stress. Central to this membrane regulation is the cardiac cytoskeleton. In the heart, the cytoskeletal network comprises a highly ordered array of structural and accessory proteins spanning from the plasma membrane to the nucleus.

Editorial see p 689
Clinical Perspective on p 708

Received February 5, 2014; accepted December 29, 2014.

From Dorothy M. Davis Heart and Lung Research Institute (S.A.S., A.C.S., J.C., C.F.K., S.C.L., I.M.B., V.P.L., M.M., I.P., L.D.H., T.R.W., P.W., R.W., P.F.B., P.M.J., A.K., R.S.H., M.S., J.M., C.A.C., T.J.H., P.J.M.), Department of Internal Medicine, Division of Cardiovascular Medicine (S.A.S., R.W., P.F.B., P.J.M.), Department of Internal Medicine, Division of Human Genetics (A.C.S., P.M.J.), Department of Physiology and Cell Biology (J.C., C.F.K., S.C.L., M.M., I.P., L.D.H., T.R.W., P.W., P.M.J., P.J.M.), and Department of Surgery (A.K., R.S.H., M.S., J.M.), The Ohio State University Wexner Medical Center; Columbus; College of Pharmacy (I.M.B., V.P.L., C.A.C.) and Department of Biomedical Engineering, College of Engineering (T.J.H.), The Ohio State University, Columbus; Division of Life Science and Institute for Advanced Study, Hong Kong University of Science and Technology, Clear Water Bay Kowloon, Hong Kong (Z.W., M.Z.); Department of Biology, South University of Science and Technology of China, Shenzhen, Guangdong, China (Z.W.); Institute of Pharmacology, Faculty of Medicine, University Duisburg-Essen, Essen, Germany (N.V., D.D.); Krannert Institute of Cardiology and Department of Medical and Molecular Genetics, Indiana University School of Medicine, Indianapolis (D.B., K.G.S., M.V.); and Department of Neuroscience, Baylor College of Medicine; Houston, TX (C.Z., M.N.R.).

The online-only Data Supplement is available with this article at http://circ.ahajournals.org/lookup/suppl/doi:10.1161/CIRCULATIONAHA.114.013708/-/DC1.

Correspondence to Peter J. Mohler, PhD, Dorothy M. Davis Heart and Lung Research Institute, 473 W. 12th Ave, DHLRI 110G, Columbus, OH 43210. E-mail peter.mohler@osumc.edu

Over the past 2 decades, the cardiac cytoskeleton has emerged as a central governing factor in the control of cardiac membrane integrity, and dysfunction in cytoskeleton and cytoskeleton-associated proteins has been directly linked to a host of human cardiac pathologies, most notably cardiac myopathies and dystrophies. In fact, human mutations in cardiac cytoskeletal or cytoskeleton-associated genes that alter myocyte signal transduction, myocardial mechanics, and force transmission are now directly linked to dilated cardiomyopathy, muscular dystrophy, and arrhythmogenic cardiomyopathy.[1–4]

In contrast to myopathy and dystrophy fields, the role of the cytoskeleton in normal cardiac electric function is not well resolved. Furthermore, until the last decade, human arrhythmia mechanisms were limited primarily to mutations in cardiac ion channels.[5] However, although literally hundreds of human variants in cardiac Na^+, K^+, and Ca^{2+} channel α and β subunits have been linked to sinus node disease, atrial fibrillation, conduction disease, and ventricular fibrillation, a second class of human arrhythmias has emerged resulting from mutations in ion channel–associated proteins, including α-syntrophin, ankyrin-G, caveolin-3, fibroblast growth factor-12, and ankyrin-B.[6] Mechanistically, dysfunction in these proteins is linked to diverse cellular pathologies, including defects in channel synthesis and membrane targeting, channel gating, and channel posttranslational modifications. Although this information has been important for new disease diagnosis and fundamental cardiac cell biology, there remain large cohorts of phenotype-positive/genotype-negative patients with familial forms of cardiac arrhythmia. Furthermore, pressing unanswered questions remain on the role for the cardiac cytoskeleton for the local organization of membrane ion channel complexes in vivo.

On the basis of genetic findings in a proband with severe ventricular arrhythmia and cardiac arrest, we uncovered a new and essential cytoskeleton-based pathway critical for cardiac electric function. We identify βII spectrin as an integral regulatory node for the organization of critical myocyte membrane and membrane-associated proteins. βII spectrin is critical for the regulation of ankyrin-B and αII spectrin, and defects in this assembly result in severe arrhythmia associated with aberrant calcium phenotypes. Moreover, we link dysfunction in this pathway to accelerated heart failure phenotypes. In summary, our findings provide a new mechanism for human excitable cell disease and uncover new roles for the cardiac cytoskeleton in human cardiovascular disease.

Methods

Statistics

Data are presented as mean±SEM. For the comparison of 2 groups, we performed Wilcoxon-Mann-Whitney *U* tests. For the comparison of >2 groups, we applied a Kruskal-Wallis test. When we obtained a significant *P* value, we continued with pair-wise comparisons using Wilcoxon-Mann-Whitney *U* tests according to the closed-testing principle. For our study, a value of $P<0.05$ was considered statistically significant.

Human Studies

Approval for use of human subjects was obtained from the Institutional Review Board of Ohio State University, and subjects provided informed consent.

Animal Studies

Procedures followed were approved and were in accordance with institutional guidelines (Ohio State University)

Additional methods are provided in the online-only Data Supplement.

Results

Identification of a New Class of *ANK2* Human Arrhythmia Mutation

Human *ANK2* variants cause cardiac arrhythmia phenotypes, including sinus node disease, atrial fibrillation, conduction block, ventricular arrhythmia, syncope, and sudden cardiac death.[7–11] We identified a new class of *ANK2* variant in a proband with a severe history of recurrent sudden cardiac arrest resulting from ventricular fibrillation (Figure 1A). The proband is a 36-year-old woman with prolonged QTc on her ECG who suffered an out-of-hospital cardiac arrest caused by ventricular fibrillation. After resuscitation, she underwent implantation of a transvenous, dual-chamber, implantable cardioverter-defibrillator. Since her first event, she has had recurrent ventricular fibrillation, resulting in syncope and implantable cardioverter-defibrillator shocks, with implantable cardioverter-defibrillator interrogation demonstrating premature ventricular complexes preceding episodes of ventricular fibrillation. In addition to prolonged QTc interval (Figure 1B), the individual displays regular premature ventricular complexes (Figure 1C), both harbingers of potential arrhythmic events. Initial genetic testing for variants in *KCNQ1*, *KCNH2*, *SCN5A*, *KCNE1*, and *KCNE2* was negative for deleterious mutations. Subsequent genetic testing using an extended sequencing panel including 5 additional genes (*ANK2*, *KCNJ2, CAV3, RYR2,* and *CASQ2*) revealed an *ANK2* c.2969G>A change, resulting in the substitution of Arg to Gln at position 990 (p.R990Q). Exon array of *ANK2* and other genes previously tested by sequencing analysis did not detect any deletions or duplications. The c.2969G>A variant is rare across multiple populations with a minor allele frequency of ≈0.007% (0 per 4406 African American alleles, 1 per 8599 European American alleles; National Heart, Lung, and Blood Institute Exome Sequencing Project). Notably, R990 is highly conserved from humans to zebrafish, roundworms, and fruit flies (Figure 1D), and structural modeling reveals that the p.R990Q variant is juxtaposed to the central ZU5 binding surface for βII spectrin (Figure 1A and 1E).[12] This region of ankyrin has not previously been linked to disease and in fact is >1500 base pairs from any previously identified variant (Figure 1A, 1D, and 1E).

Ankyrin-B and βII Spectrin Are Molecular Partners in Human Heart

A requisite function of a canonical ankyrin polypeptide is association with the α/β spectrin heterotetramer. This complex, by association with actin (via spectrin), functionally couples integral membrane proteins (ion channels, receptors, transporters) with the cytoskeletal infrastructure. Ankyrins associate with β spectrin gene products through conserved residues in the N-terminal ZU5 (Zu5N) domain.[12] On the basis of the location of the human variant, we tested the functional relationship

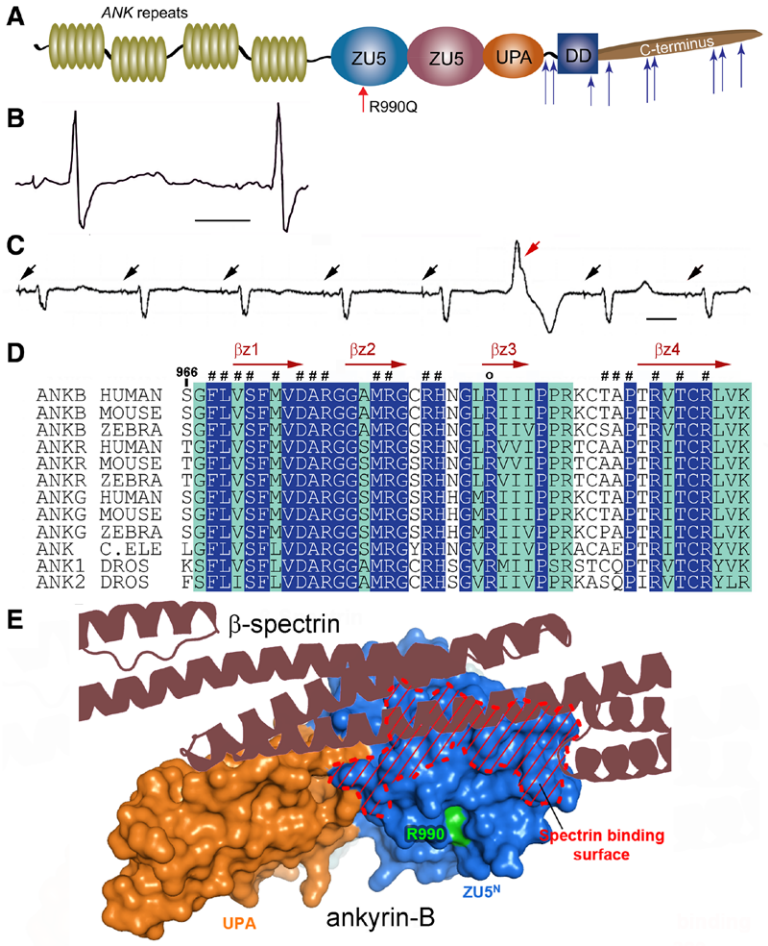

Figure 1. Ankyrin-B arrhythmia variant identified in conserved spectrin-binding domain. **A**, Ankyrin-B includes *ANK* repeats, a spectrin-binding domain comprising 2 ZU5 and 1 UPA domain, and a regulatory domain comprising a death and C terminus. Identified *ANK2* loss-of-function mutations are noted by blue arrows, and the novel p.R990Q variant is indicated in red. **B**, *ANK2* p.R990Q proband displays QT prolongation. **C**, A 10-second rhythm strip in the p.R990Q proband demonstrating atrial demand pacing (black arrows) with premature ventricular contraction (red arrow). **D**, Sequence alignment of ankyrin-B spectrin-binding sequence. Residues that are absolutely conserved and highly conserved are in blue and green, respectively. Secondary structural elements are indicated above the alignment. p.R990Q is conserved across species and marked with "o." **E**, Structure of the $ZU5^N$-UPA tandem of ankyrin-B spectrin-binding domain reveals the spectrin-binding surface and location of p.R990 (green).

between ankyrin-B and βII spectrin. βII spectrin is normally localized at myocyte T tubules (Figure 2A and Figure I in the online-only Data Supplement) with ankyrin-B.[13] Ankyrin-B directly associates with radiolabeled βII spectrin (Figure 2B), and βII spectrin coimmunoprecipitates with ankyrin-B from detergent-soluble lysates from adult mouse heart and nonfailing human heart (Figure 2C and 2D). We observed a larger macromolecular complex between ankyrin-B and βII spectrin with membrane proteins, including the Na^+/K^+ ATPase and Na^+/Ca^{2+} exchanger (ankyrin-binding partners), as well as the cytoskeletal element actin by coimmunoprecipitation experiments from both mouse and human heart (Figure 2C and 2D). These data demonstrate the presence of a βII spectrin/ankyrin-B cytoskeletal complex in heart.

We hypothesized that the human p.R990Q variant confers susceptibility to cardiac arrhythmia by altering ankyrin-B binding for βII spectrin, thus affecting integration of membrane proteins with the cytoskeleton.[12,14] Whereas wild-type ankyrin-B robustly associated with βII spectrin, we observed a significant decrease in binding of ankyrin-B p.R990Q with βII spectrin (Figure 2E and 2F). In silico modeling for the human p.R990Q variant with the costructure for ankyrin-B and βII spectrin revealed that the R990 forms several hydrogen bonds and salt bridges with surrounding residues, a property strictly conserved in all ankyrins (Figure 2G). Moreover, modeling revealed that p.R990Q results in loss of salt bridge interactions with surrounding residues (Figure 2G). Ankyrin-B p.R990Q may directly disrupt βII spectrin binding. Alternatively, on the basis of the localization of the residue, this mutation may destabilize the folding of the ZU5 domain, resulting indirectly in the loss of spectrin binding and overall loss of ankyrin-B function.

Analysis of Human Variants That Block βII Spectrin Binding in Myocytes

We tested the relationship between human ankyrin-B variants and βII spectrin in primary myocytes. Because mice lacking global ankyrin-B expression die in utero or shortly after birth, thus limiting the ability to study ankyrin-dependent mechanisms past postnatal day 2, we generated a new mouse model homozygous for a conditional cardiac ankyrin-B–null allele (αMHC-Cre; ankyrin-B conditional knockout [cKO] mouse; Figure II in the online-only Data Supplement). The null allele was created by targeting *Ank2* exon 24 disrupting all known *Ank2* splice products. The mutant allele was confirmed by Southern blot and polymerase chain reaction strategies (Figure IIB in the online-only Data Supplement), and myocytes from ankyrin-B cKO mice display loss of ankyrin-B protein by immunoblot and immunostaining (Figure IIC–IIF in the online-only Data Supplement). Using well-differentiated primary neonatal ankyrin-B cKO myocytes (postnatal day 7), we tested the

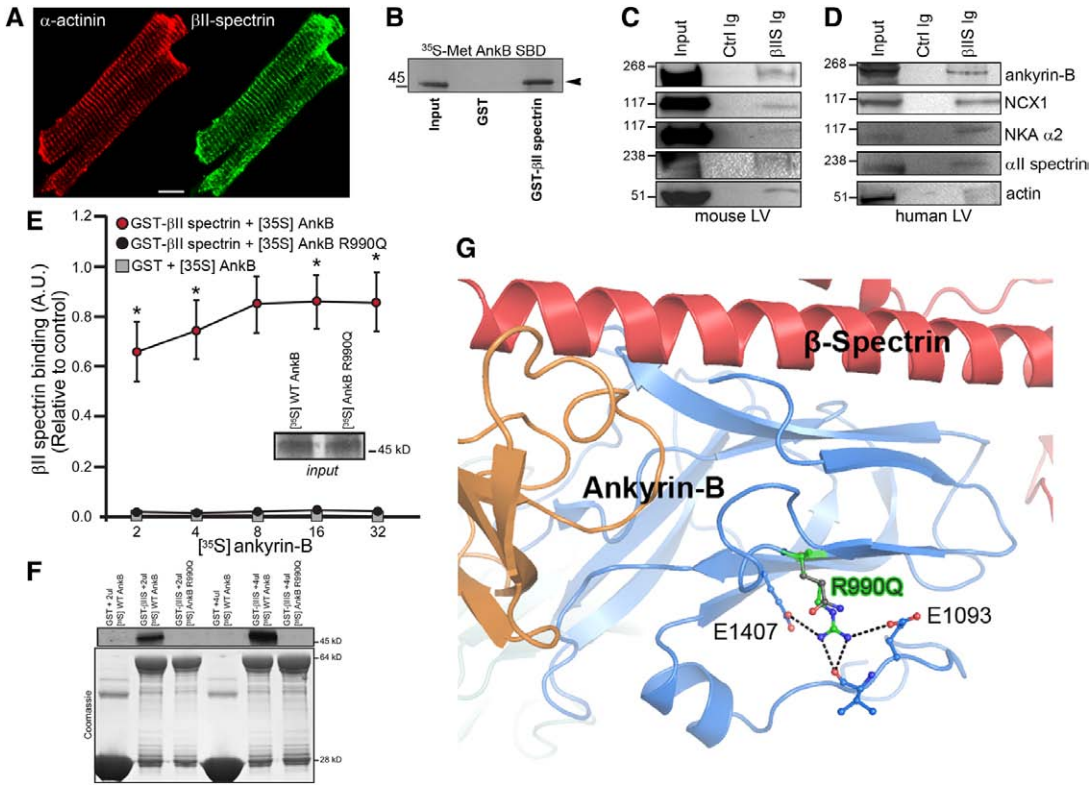

Figure 2. Ankyrin-B/βII spectrin complex is blocked by human disease mutation. **A**, βII spectrin (green) is localized in a striated pattern in isolated mouse myocytes (colabeled with α-actinin, red). Scale, 10 μm. **B**, Radiolabeled ankyrin-B (spectrin-binding domain) associates with GST βII spectrin fusion protein but not GST. **C** and **D**, βII spectrin (β_{II}S) Ig coimmunoprecipitates ankyrin-B, NCX1, Na/K ATPase, αII spectrin, and actin from detergent-soluble lysates of nonfailing mouse and human left ventricle (LV). **E**, Human *ANK2* p.R990Q arrhythmia variant displays aberrant βII spectrin binding. Data in inset represent equal inputs for experiments. Curves denote binding for GST-βII spectrin or GST alone with a concentration range of radiolabeled ankyrin-B or radiolabeled ankyrin-B R990Q (n=5 per group; **P*<0.05). **F**, Primary binding data and Coomassie Blue–stained gels for fusion proteins in **E**. **G**, Ribbon structure from co-crystal structure of ankyrin-B/βII spectrin. Human p.R990Q variant shown in green.

activity of the p.R990Q variant. Wild-type ankyrin-B–green fluorescent protein or human ankyrin-B variant p.R990Q was introduced into ankyrin-B cKO myocytes. Notably, compared with control wild-type myocytes (Figure IIIA and IIIB in the online-only Data Supplement), ankyrin-B cKO myocytes display loss of targeting of Na^+/Ca^{2+} exchanger, a known binding partner in heart (Figure IIIC and IIID in the online-only Data Supplement). Green fluorescent protein–ankyrin-B was striated when expressed in ankyrin-B cKO myocytes and was sufficient to rescue the localization of the Na^+/Ca^{2+} exchanger (Figure IIIE and IIIF in the online-only Data Supplement). In contrast, ankyrin-B p.R990Q, similar to 2 ankyrin-B mutants previously identified as lacking spectrin binding (A1000P and DAR976AAA),[13] was not appropriately targeted (diffuse cytoplasmic expression) and failed to rescue the localization of the Na^+/Ca^{2+} exchanger (Figure IIIG–IIIL in the online-only Data Supplement).

βII Spectrin cKO Mice Display Sinus Node Dysfunction and Ventricular Arrhythmia

The functional role for βII spectrin for postnatal cardiac function in vivo is unknown and untested. We therefore examined cardiac electric phenotypes in a new mouse model with conditional deletion of cardiac βII spectrin (βII spectrin cKO; Figure 3A). βII spectrin cKO mice lack βII spectrin in heart but not in other tissues (Figure 3B–3F). Telemetry studies of conscious mice show reduced heart rate, increased heart rate variability, atrioventricular block, and proarrhythmic ECG phenotypes (widened QRS complexes, prolonged QT interval) in βII spectrin cKO mice compared with wild-type littermates at baseline (Figure 4A–4H). Notably, catecholaminergic stress (exercise or low-dose epinephrine) resulted in pronounced ventricular arrhythmia (both nonsustained and sustained episodes) and death (Figure 4L–4N). We observed no difference in maximal heart rate in response to low- or high-dose epinephrine (Figure IV in the online-only Data Supplement), and under no circumstances were ECG or arrhythmic anomalies observed in control littermates. Although cardiac electric dysfunction may arise secondary to structural heart disease (hypertrophy, heart failure), we observed no significant differences in mean left ventricular ejection fraction, cardiac output, wall thickness, or other significant structural phenotypes between control and βII spectrin cKO mice (Figures VA, VB, and VIA–VIM in the online-only Data Supplement).

βII Spectrin cKO Myocytes Display Afterdepolarizations and Abnormal Calcium Waves

On the basis of the severity of observed arrhythmias in βII spectrin cKO mice, we examined βII spectrin cKO mouse

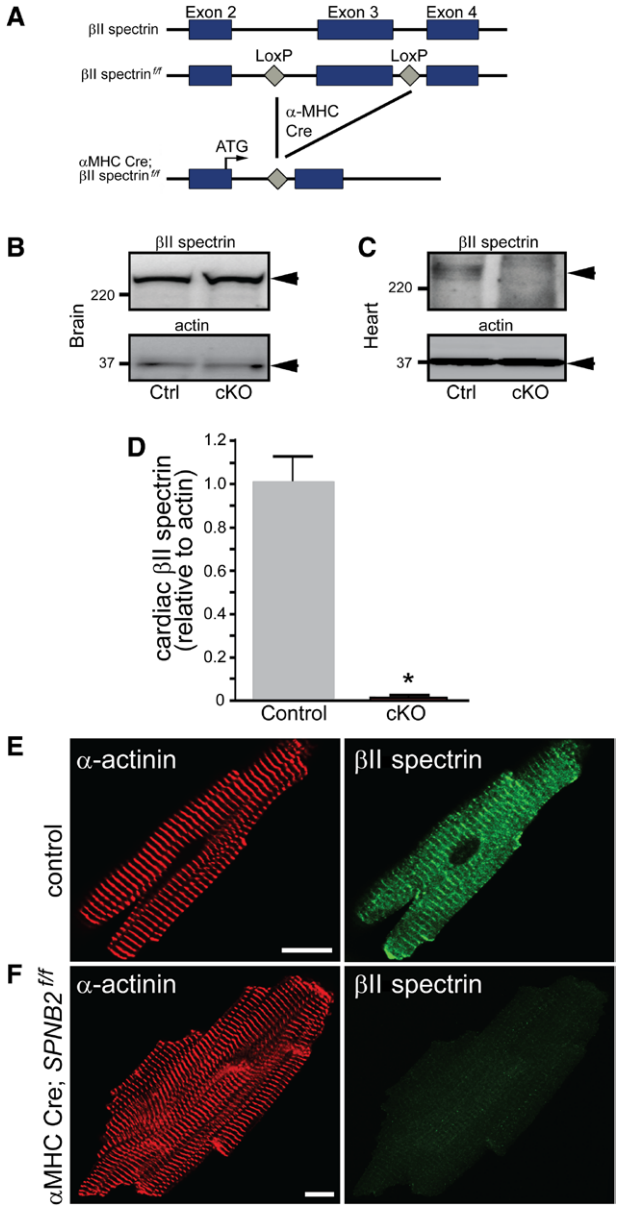

Figure 3. Generation and validation of mice lacking βII spectrin in cardiomyocytes. **A**, Targeting strategy to generate Cre-dependent loss of cardiac βII spectrin. βII spectrin in brain (**B**) and heart (**C**) of control and βII spectrin conditional knockout (cKO) mice. **D**, βII spectrin levels in control (n=5) vs βII spectrin cKO (n=5; $P<0.05$) hearts. **E**, βII spectrin localization in control and βII spectrin cKO adult ventricular myocytes. Bar=10 μm. α-MHC indicates α-myosin heavy chain.

ventricular myocyte action potentials. Unlike myocytes from control littermates, βII spectrin cKO myocytes displayed chaotic electric behavior even in the absence of catecholamine stimulation (Figure 5A and 5C). Mean APD_{90} was not different between genotypes (Figure 5I). However, we observed frequent spontaneous afterdepolarizations in βII spectrin cKO myocytes at baseline (Figure 5C and 5D). Afterdepolarizations were present independently of pacing frequency and increased in both frequency and duration after superfusion with isoproterenol (Figure 5B, 5D, and 5F). We tested whether spontaneous calcium release potentially underlies the chaotic electric behavior of βII spectrin cKO myocytes by examining action potentials in the presence of ryanodine, an inhibitor of Ca^{2+} release from the sarcoplasmic reticulum (SR). Notably, ryanodine (100 nmol/L) prevented afterdepolarizations in myocytes with or without isoproterenol (Figure 5G, 5H, and 5J). Together, these data strongly support a critical role for βII spectrin in regulating myocyte electric behavior and suggest a role for intracellular Ca^{2+} as a potential mechanism underlying the electric arrhythmogenic phenotypes.

Spontaneous Ca^{2+} waves (SCaWs) at the level of the myocyte may mediate Ca^{2+}-dependent afterdepolarizations, known cellular triggers for arrhythmia.[15,16] Therefore, we compared the relative propensity of control and βII spectrin cKO myocytes to generate SCaWs. βII spectrin cKO myocytes were significantly more likely to generate SCaWs compared with control myocytes (Figure 5M–5Q). SCaWs were observed in ≈56% of βII spectrin cKO myocytes compared with only ≈18% of control myocytes (Figure 5K), and we observed <0.2 waves per wild-type myocyte versus an average of ≈2 waves per βII spectrin cKO myocyte ($P<0.05$). Importantly, spontaneous unified Ca^{2+} release events (indicated by a perpendicular spontaneous dye front in the confocal line scans) were frequently observed in βII spectrin cKO myocytes but not in control myocytes (Figure 5O–5Q). Such perpendicular waves are indicative of a unified Ca^{2+} release within the myocyte and provide evidence that the cell spontaneously reached the threshold that initiated an action potential. Such a unified spontaneous Ca^{2+} release was not observed in control myocytes; rather, only slowly propagating waves were observed (Figure 5M). This SCaW-dependent phenotype provides a mechanism for the afterdepolarizations observed in βII spectrin cKO myocytes.

βII Spectrin Is Required for the Organization of Cardiac Membrane Proteins

We hypothesized that loss of normal calcium cycling and arrhythmias in βII spectrin cKO mice reflected the central role for βII spectrin in organizing cardiac membrane proteins. To test this hypothesis, we first examined the status of T-tubule and SR membrane proteins critical for calcium release. Although we observed no difference in T-tubule L-type calcium channel localization or T-tubule structure between genotypes (Figure 6A and 6B), we observed heterogeneity in the subcellular localization of ryanodine receptor 2 (RyR_2), the primary cardiac SR calcium release channel in βII spectrin cKO myocytes (Figure 6D and Figure VII in the online-only Data Supplement). To further examine potential RyR_2 heterogeneity, we analyzed RyR_2 localization by total internal reflection fluorescence and superresolution imaging (see Methods in the online-only Data Supplement). In agreement with the previous superresolution imaging of Baddeley and colleagues,[17] RyR_2 is localized by these techniques to discrete clusters of irregular shapes and sizes (Figure 6E). In contrast, RyR_2 imaging of heterogeneous regions of interest (ie, red asterisk in Figure 6D, right) in βII spectrin cKO myocytes showed reduced size and intensity of RyR_2 clusters, as well as irregular intensity patterning, compared with control myocytes (Figure 6F). Consistent with these findings,

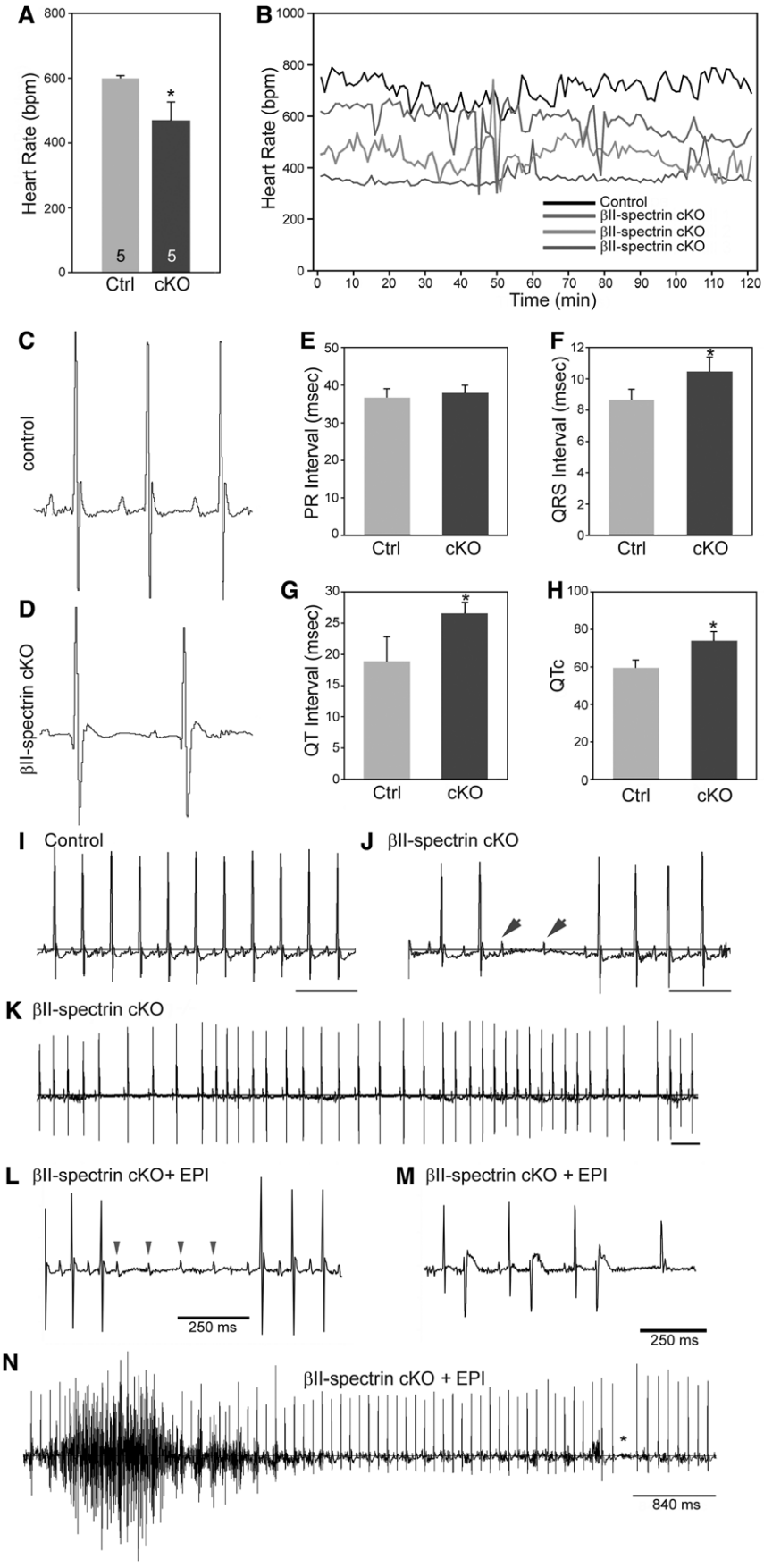

Figure 4. Loss of βII spectrin causes bradycardia, rate variability, and arrhythmia. **A** and **B**, βII spectrin conditional knockout (cKO) mice display reduced heart rate (n=5) as assessed by telemetry compared with control mice (n=5; $P<0.05$). **B**, Heart rates of control and 3 βII spectrin cKO mice that show bradycardia and rate variability. **C** and **D**, ECGs from control and βII spectrin cKO mouse showing increased RR, QRS, and QT intervals. Mean data for parameters are shown in **E** through **H** (n=5 mice per genotype; $P<0.05$). **I** and **J**, Control ECG recording over 1 second demonstrating no R-R variability or heart block vs ECG recording from a βII spectrin cKO littermate demonstrating type II heart block, confirmed by P waves (arrowheads) without ventricular conduction. **K**, A 3-second ECG recording of a βII spectrin cKO mouse demonstrating significant R-R variability with heart block. **L** through **N**, βII spectrin cKO mice demonstrate severe arrhythmia phenotypes and death after injection of epinephrine (EPI). Examples include (**L**) 4 sinus P waves (arrowheads) without ventricular conduction, consistent with type II atrioventricular block, (**M**) bigeminy, and (**N**) polymorphic ventricular arrhythmia.

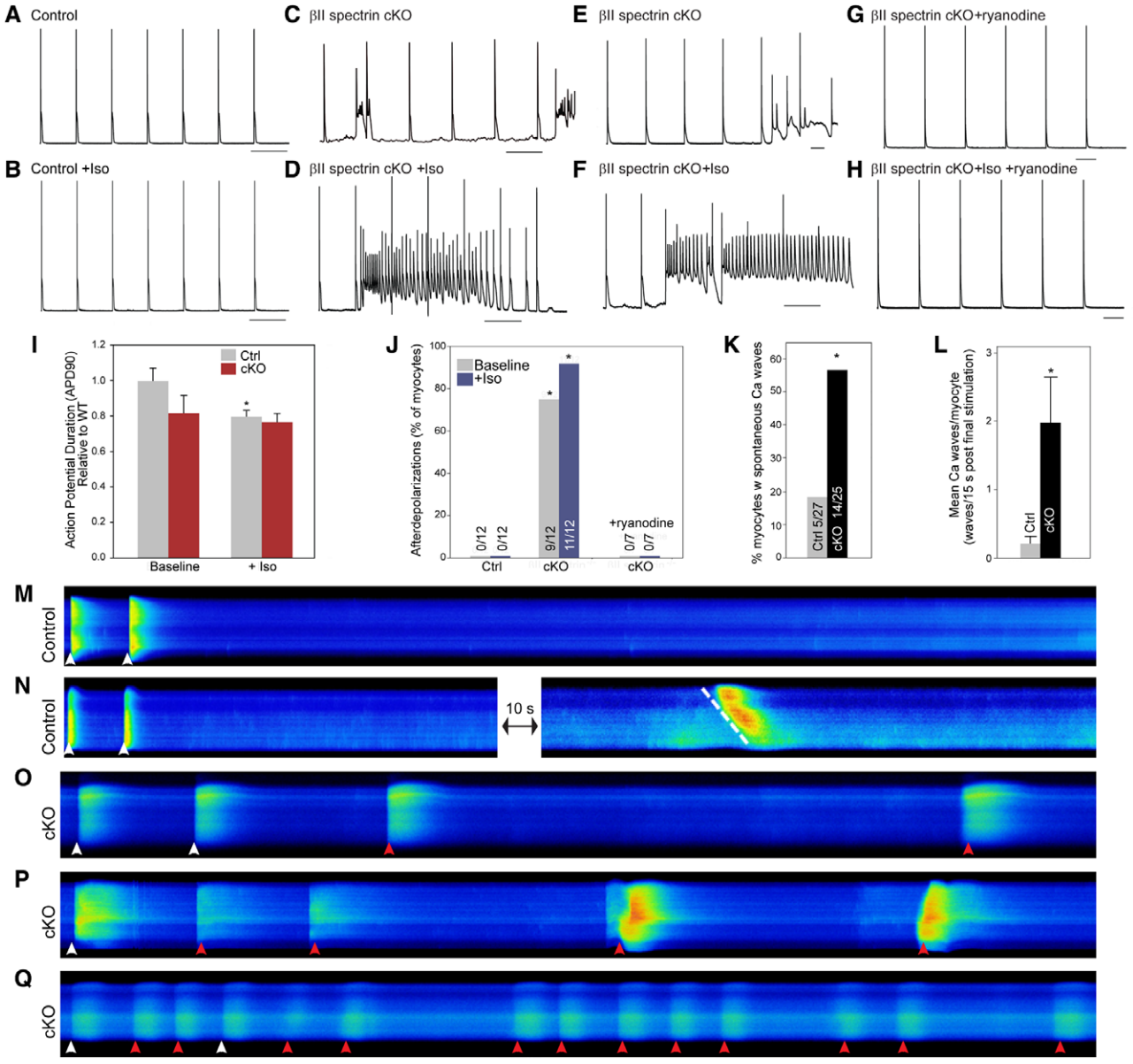

Figure 5. βII spectrin conditional knockout (cKO) myocytes display electric instability, afterdepolarizations, and aberrant Ca waves. Action potential measurements of (**A** and **B**) control and (**C** and **D**) βII spectrin cKO myocytes measured at baseline at 0.5-Hz pacing protocol with or without 1 μmol/L isoproterenol (Iso). **E** and **F**, Electric instability was present in βII spectrin cKO myocytes independently of pacing frequency (shown at 1 Hz). **G** and **H**, Ryanodine (100 nmol/L) blocked abnormal electric instability of βII spectrin cKO myocytes with or without Iso. **I**, Mean APD_{90} of control and βII spectrin cKO myocytes with or without Iso (n>10 myocytes per genotype; $P<0.05$ for control vs control+Iso). **J**, Prevalence of afterdepolarizations for control and βII spectrin cKO myocytes with or without Iso and in the presence of ryanodine (n>10 myocytes per treatment; $P<0.05$ for control vs cKO at baseline; $P<0.05$ for control+Iso vs cKO+Iso). **K** and **L**, βII spectrin cKO myocytes were more likely to form spontaneous Ca^{2+} waves (n=27 control, n=25 βII spectrin cKO; $P<0.05$). **M** through **Q**, Line-scan images of fluo-4–loaded myocytes field stimulated at 0.5 Hz. After stimulation, myocytes were continuously monitored for spontaneous Ca^{2+} wave formation for 15 seconds. **M** and **N**, Control myocytes with no spontaneous wave activity. When waves formed, they were slow moving (**N**, dashed white line). **O** through **Q**, Spontaneous waves in βII spectrin cKO myocytes (red arrowheads). Stimulated transients are indicated by white arrowheads. WT indicates wild-type.

RyR_2 levels were significantly reduced in βII spectrin cKO hearts (Figure 6G and 6H). This loss was selective for RyR_2 compared with other SR proteins in that we observed no difference in the expression or localization of the SR calcium ATPase or in the intercalated disk protein N-cadherin (Figure 6C). In summary, these data define βII spectrin as required for the selective local organization of RyR_2 calcium release channels. Of note, defects in local RyR_2 organization have been linked to aberrant calcium-dependent release, arrhythmia, and heart failure phenotypes in humans and animal models.[18–20]

βII spectrin Is Required for the Expression and Targeting of Ankyrin-B

In addition to RyR_2, βII spectrin cKO mice displayed loss of expression and localization of ankyrin-B in adult heart

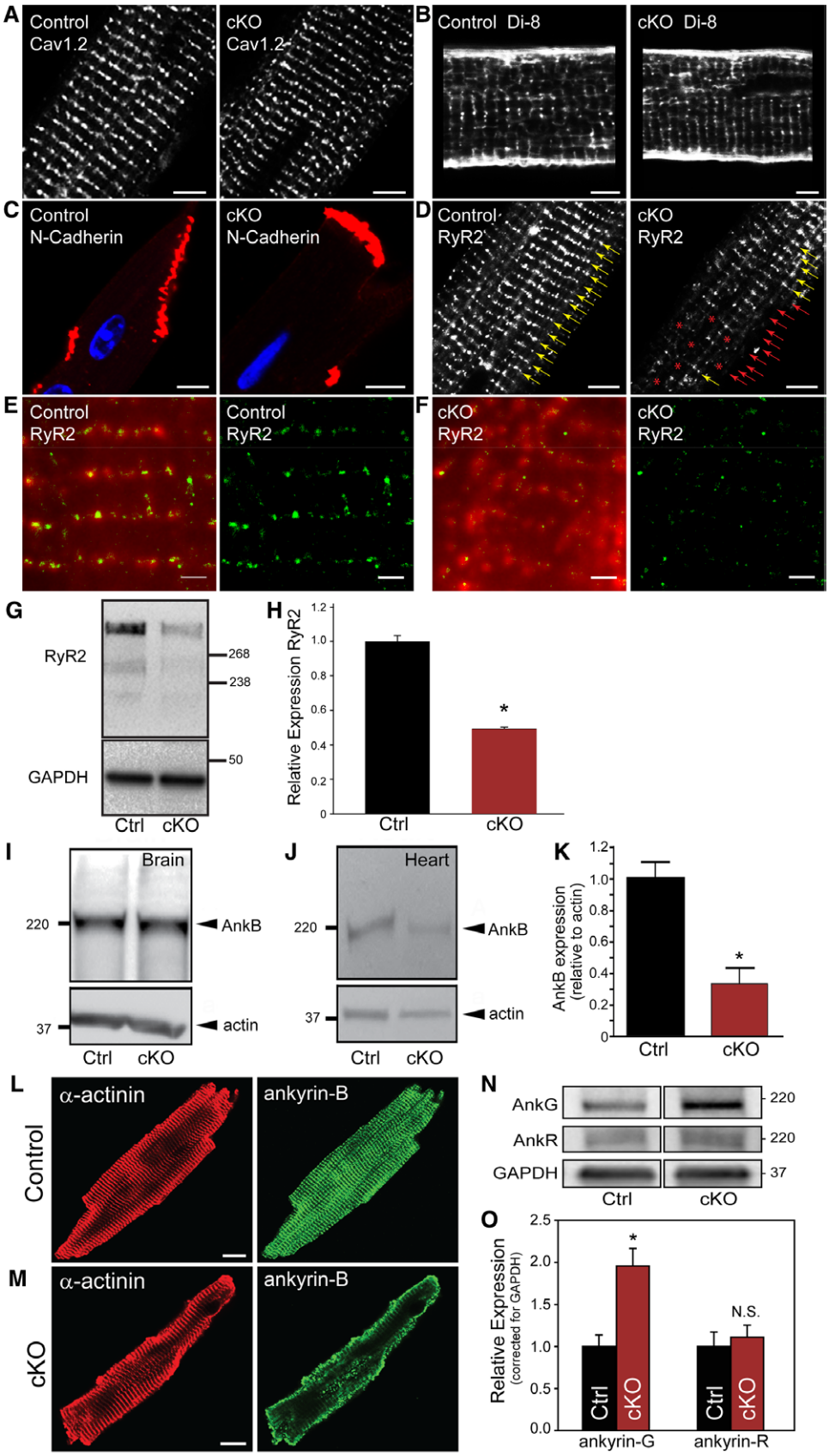

Figure 6. βII spectrin is required for organization of calcium release units and ankyrin-B. Like control mouse myocytes, βII spectrin conditional knockout (cKO) myocytes display normal localization of transverse tubule $Ca_v1.2$ (**A**), transverse tubule organization (**B**; visualized by Di-8-ANEPPs), and intercalated disk N-cadherin (**C**). In contrast, ryanodine receptor 2 (RyR_2) expression was reduced and heterogeneous in βII spectrin cKO myocytes (**D**, red asterisk). **E** and **F**, RyR_2 expression was further analyzed by total internal reflection (*continued*)

(Figure 6I–6M). These findings were initially unanticipated because prior work implicates ankyrin-B as critical for βII spectrin targeting and localization in postnatal day 2 neonatal cardiomyocytes.[13] To define the functional relationship of ankyrin-B and βII spectrin in myocyte localization, we evaluated βII spectrin and ankyrin-B localization in wild-type neonatal cardiomyocytes. As shown in Figure VIII in the online-only Data Supplement, striated expression of ankyrin-B precedes βII spectrin at postnatal day 1 in mice. However, both proteins are expressed and colocalized by postnatal day 3 (Figure VIII in the online-only Data Supplement). In support of a role of ankyrin-B in the targeting of βII spectrin and in agreement with prior work,[13] ankyrin-B cKO neonatal cardiomyocytes lack βII spectrin expression or striation at postnatal day 1 or 3 (Figure VIII in the online-only Data Supplement). However, we were surprised to observe that, later in myocyte maturation (postnatal day 7), ankyrin-B expression was not requisite for βII spectrin expression. In fact, βII spectrin expression in postnatal day 7 myocytes is equivalent to the expression/staining observed in wild-type cardiomyocytes (Figure VIII in the online-only Data Supplement). This is further illustrated in adult myocytes in which we observe no difference in βII spectrin expression or localization in ankyrin-B cKO hearts (Figures IX and X in the online-only Data Supplement). Finally, βII spectrin cKO cardiomyocytes demonstrate normal expression and localization of ankyrin-B at postnatal day 1 and 3 but loss of ankyrin-B expression and targeting at postnatal day 7 (Figure VIII in the online-only Data Supplement). Together, these findings demonstrate a complex relationship between ankyrin and βII spectrin in heart. More specifically, our data show that ankyrin-B plays a dominant role for βII spectrin targeting in immature, developing myocytes, whereas in maturing and mature myocytes, βII spectrin assumes the dominant targeting role for ankyrin-B. Although we assume that this transition likely represents a shift in the maturity of the membrane/cytoskeletal network (ie, myocyte transverse tubules begin to develop ≈7 days in culture),[21] future work will be important to better define the underlying mechanisms. Notably, although βII spectrin cKO mice displayed reduced ankyrin-B expression, we observed no change in the expression of ankyrin-R (*Ank1*) in βII spectrin cKO adult heart compared with control heart (Figure 6N and 6O). However, ankyrin-G (*Ank3*), a third ankyrin gene product expressed in heart,[22] showed elevated expression in βII spectrin cKO hearts (Figure 6N and 6O), likely as a compensatory mechanism in response to reduced ankyrin-B levels.

βII Spectrin Is Required for Organization of Ankyrin-B–Associated Membrane Proteins

Ankyrin-B targets Na^+/Ca^{2+} exchanger and Na^+/K^+ ATPase and controls regulation of dyadic proteins, including RyR_2.[23] Consistent with our above findings, we observed a significant decrease in I_{NCX} in βII spectrin cKO myocytes (Figure 7A and 7B). These changes were confirmed by both immunoblot and immunostaining in which we observed decreased expression of the Na/Ca exchanger and Na/K ATPase (Figure 7C–7E). Notably, despite the major alterations in electric activity in βII spectrin cKO myocytes, we did not observe differences in I_{Na} current (peak, activation/inactivation/late current) and $Na_v1.5$ and connexin43 protein levels were unchanged in βII spectrin cKO hearts (Figure 7C and Figure XI in the online-only Data Supplement). Together with our data on RyR_2, these findings identify βII spectrin as essential for the localization of multiple membrane proteins required for myocyte Ca^{2+} regulation.

βII Spectrin Regulates αII Spectrin and the Myocyte Microtubule Network

Whereas the Na/Ca exchanger and Na/K ATPase loss is likely related to loss of ankyrin-B targeting in βII spectrin cKO mice, the mechanism for RyR_2 dysfunction is less clear. We hypothesized that this defect reflects an important role for βII spectrin in organizing local cardiac cytoskeleton. In metazoans, α and β spectrin form a submembrane lattice through formation of heterotetramers via antiparallel N- and C-terminal interactions. However, the requirement of βII spectrin expression for the targeting and formation of the heterotetramer in heart is unknown. We examined the abundance of αII spectrin, an in vivo partner for cardiac βII spectrin. Consistent with prior reports demonstrating degradation of α spectrin in the absence of adequate erythroid β spectrin,[24–26] αII spectrin levels were reduced nearly 50% in βII spectrin cKO hearts (Figure 7F and 7G). In line with these data, we observed a reduced abundance of αII spectrin in βII spectrin cKO myocytes by immunostaining (Figure 7H–7K). On the basis of these data, we further investigated the integrity of the cytoskeleton in βII spectrin cKO myocytes. Although actin was unchanged in the expression or localization in βII spectrin cKO mice, we observed significant increases in levels of βI spectrin and α and β tubulin in βII spectrin cKO hearts by immunoblot or immunostaining (Figure 7L–7O and Figure XII in the online-only Data Supplement), likely as a compensatory response to βII spectrin deficiency and consistent with prior findings of tubulin remodeling in failing hearts.[27] However, levels of desmin, an intermediate filament protein critical for myocyte cytoskeletal

Figure 6 (*continued*). fluorescence (TIRF) and superresolution imaging. **E** and **F**, Left, Overlay of a TIRF image (red) and the corresponding superresolution image (green) of RyR_2 in control (**E**) and βII spectrin cKO (**F**) cardiomyocytes. **E** and **F**, Right, Superresolution images of RyR_2 in control and βII spectrin cKO myocytes. Note that data in **F** were collected from an area of RyR_2 heterogeneity (red asterisk, cKO panel **D,** right) that illustrates reduced RyR_2 cluster size and intensity. Scale bar for **E** and **F**, 1000 nm. **G** and **H**, RyR_2 levels were significantly reduced in βII spectrin cKO myocytes (n=4 hearts per genotype; $P<0.05$). **I** through **K**, Ankyrin-B levels are decreased in the heart but not brain of βII spectrin cKO mice (n=5 hearts per genotype; $P<0.05$). **L** and **M**, Ankyrin-B shows reduced expression and abnormal targeting in βII spectrin cKO vs control myocytes (scale bar, 10 μm). **N** and **O**, Ankyrin-G but not ankyrin-R levels are decreased in the heart of βII spectrin cKO mice (n=5) vs control mice (n=6; $P<0.05$).

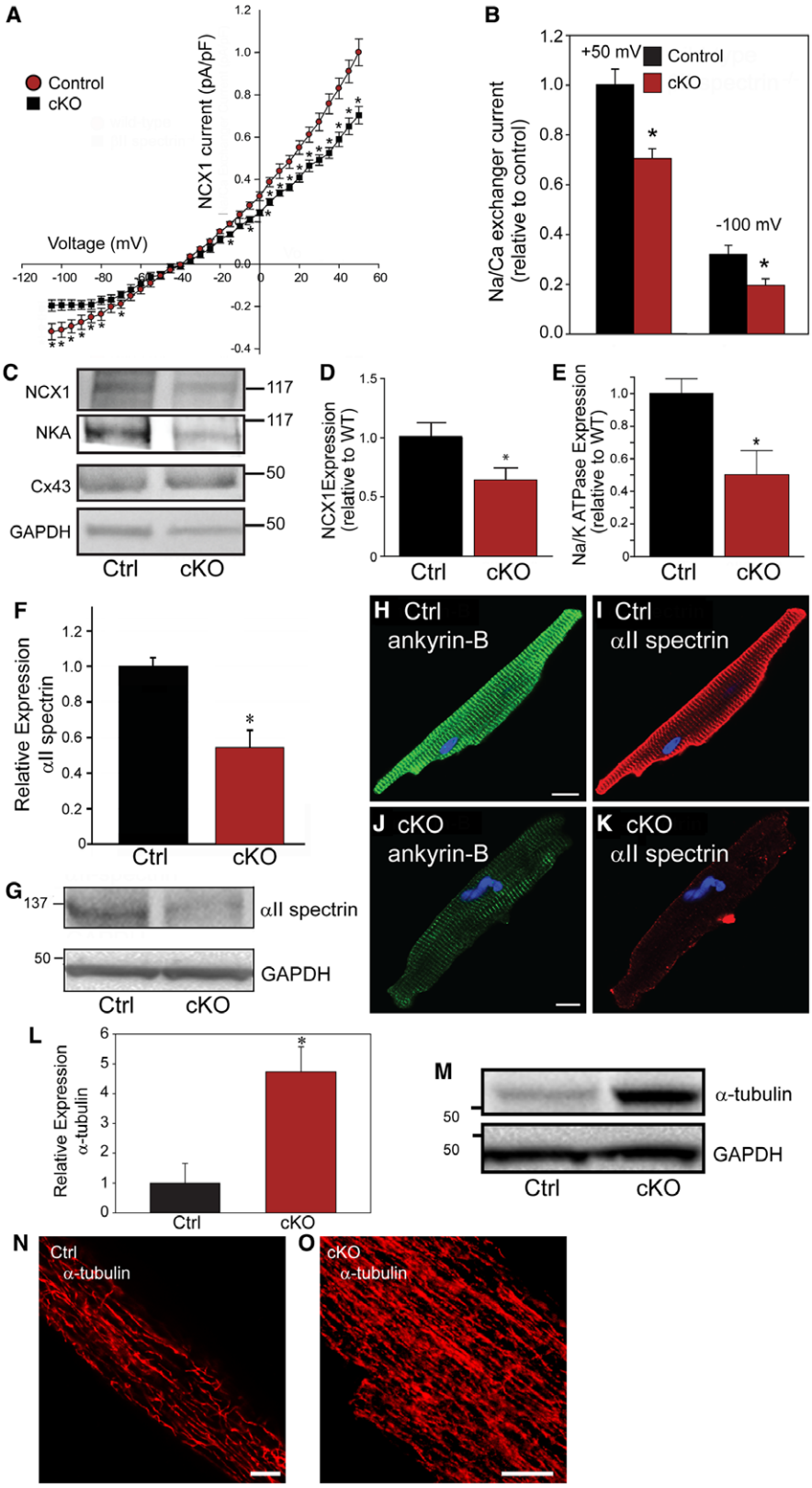

Figure 7. βII spectrin deficiency results in reduced expression of ankyrin-B–associated membrane proteins and abnormal myocyte cytoskeletal organization. **A** and **B**, βII spectrin conditional knockout (cKO) myocytes (n=12) display reduced I_{NCX} compared with control mouse myocytes (n=14; $P<0.05$). **C** through **E**, βII spectrin cKO hearts display reduced Na/Ca exchange (NCX) and Na/K ATPase expression but normal expression of connexin43 (Cx43) compared with control hearts (n=4 hearts per genotype; $P<0.05$). **F** through **K**, βII spectrin cKO hearts (n=5) display reduced αII spectrin expression and localization compared with control hearts (n=5) by immunoblot and immunostaining ($P<0.05$). **L** through **O**, βII spectrin cKO hearts display a significant increase in α-tubulin expression by immunoblot and immunostaining with control hearts (n=5 hearts per genotype for **L**; $P<0.05$). Scale bar, 10 μm for **N** and **O**.

infrastructure, were unchanged between control and βII spectrin cKO hearts (Figure XII in the online-only Data Supplement). In summary, these data demonstrate that myocytes lacking βII spectrin display significant yet selective cytoskeletal remodeling.

βII Spectrin cKO Mice Display Accelerated Heart Failure Phenotypes

Heart failure is characterized by significant electric and structural remodeling. On the basis of severe electric and structural phenotypes present in βII spectrin cKO mice at baseline, we hypothesized that βII spectrin cKO mice would display accelerated and more pronounced cardiac damage after induction of heart failure through transverse aortic constriction. Notably, unlike control littermates or sham βII spectrin cKO mice, βII spectrin cKO mice displayed cardiac arrhythmia and death associated with major structural remodeling after 6 weeks of banding (Figure 8A–8G). Examination of βII spectrin cKO mouse banded sections revealed a high prevalence of widespread myocardial degeneration of the left ventricular free wall and septum that was characterized by vacuolation, pallor, and interstitial and ventricular myocyte necrosis (Figure 8A–8D). Furthermore, at 6 weeks after banding, βII spectrin cKO mice displayed severe atrioventricular block, ST-segment depression, frequent premature ventricular complexes, and junctional rhythms (Figure 8E–8G). Although we observed standard pre–heart failure phenotypes in control mice in response to the transverse aortic constriction protocol, we did not observe the extensive electric or structural phenotypes found in βII spectrin cKO littermates.

Discussion

The spectrin superfamily is composed of 2 α spectrin and 5 β spectrin genes. Most information on spectrin function comes from the erythrocyte, although a growing body of literature points to key roles of spectrin family members in cytoskeletal infrastructure in complex cells. In the red blood cell, α and β spectrin tetramerize and form the basis of the submembrane ultrastructure through interactions with membrane proteins (eg, anion exchanger) and cytoskeleton (actin). Mutations in α or β spectrin in humans or animals result in loss of membrane integrity, spherocytosis, and hemolytic anemia.[28] In fact, spectrin mutations are the cause of the most common forms of hereditary spherocytosis in the white population. In complex cells, spectrins are critical for membrane assembly and maintenance, and both αII and βII spectrin–deficient mice are embryonic lethal.[29,30] βII spectrin is required for lateral membrane formation of columnar epithelial cells in the lung,[31] and βII spectrin and βIV spectrin are critical for the development and maintenance of the axon initial segment and nodes of Ranvier in the central nervous system.[32–34] Little is known about the role of βII spectrin in heart because mice homozygous for βII spectrin allele deficiency die in utero.[30] However, data from the βIII spectrin literature offer insight into the likely mechanisms for βII spectrin function in heart. For example, work from Armbrust et al[35] and Stankewich and colleagues[36] demonstrates that βIII spectrin is essential for membrane protein targeting in the nervous system. Similar to our findings in heart, targeted deletion of βIII spectrin in brain results in impaired assembly of the postsynaptic membrane, endomembrane retention of multiple synaptic proteins, and ataxia and seizure phenotypes.[36] Moreover, human βIII spectrin gene mutations found in the region where βIII spectrin

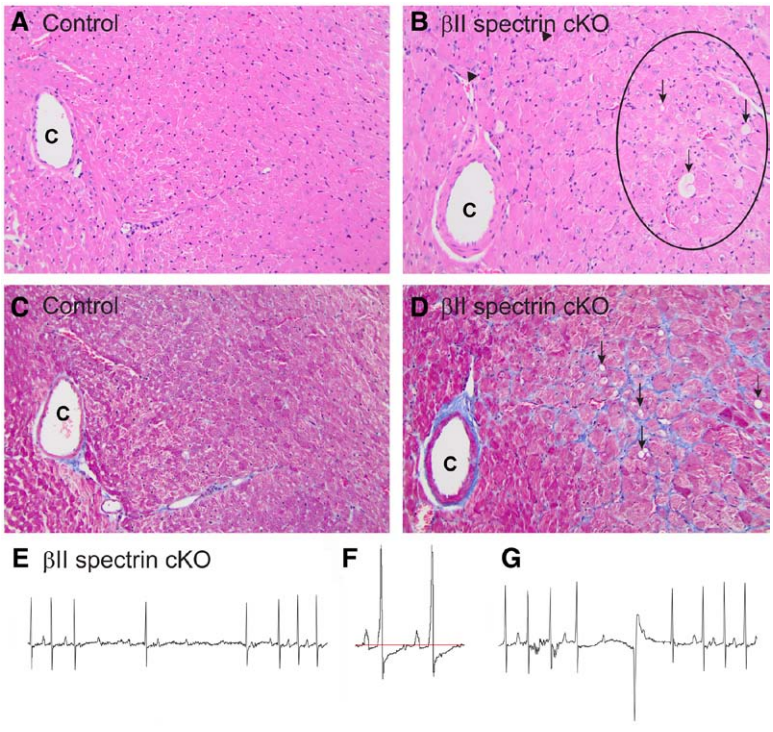

Figure 8. βII spectrin conditional knockout (cKO) mice show severe damage and electric phenotypes after aortic banding. **A** and **B**, Unlike control transverse aortic constriction mice, βII spectrin cKO mice displayed widespread myocardial degeneration of the left ventricular free wall and septum, characterized by vacuolation (arrows), pallor (inside circle), and necrosis of myocytes (hematoxylin and eosin staining; magnification, ×200). **C** and **D**, βII spectrin cKO hearts further displayed increased interstitial fibrosis (blue) of connective tissue compared with control sections (vacuolation noted by arrows; magnification, ×200). Electric phenotypes observed in βII spectrin cKO and not control mice included (**E**) atrioventricular conduction defects, (**F**) ST-segment depression, and (**G**) intermittent premature ventricular complexes and junctional beats. C indicates coronary artery.

associates with the dynactin subunit Arp1[37] cause human spinocerebellar ataxia (SCA5) resulting from defects in membrane protein (glutamate transporter EAAT4, metabotropic glutamate receptor 1α) targeting.[35,38] Thus, from the βIII spectrin data and our new findings, we hypothesize that βII spectrin is a critical player in membrane protein sorting instead of simply a static membrane structural protein. In fact, the demonstrated links between spectrins and dynactin[37] provide a logical rationale for the cell and molecular phenotypes observed in βII spectrin cKO animals. Although this study focused on the relationship between βII spectrin and ankyrin-B, our new data (Figure 6N and 6O) indicate that it will be important to identify the relationship of βII spectrin with other cardiac ankyrin and spectrin gene products.

An important but unexpected finding of this study is the essential role of βII spectrin for the local organization of RyR_2. Cardiac RyR_2 is a central player for myocyte calcium release, and RyR_2 dysfunction has been linked to a broad spectrum of heart failure and arrhythmia phenotypes in human and animal models.[39–42] Our data demonstrate a role of βII spectrin for both the expression and targeting of RyR_2. However, potentially more significant, remaining RyR_2 populations in βII spectrin cKO myocytes are disorganized, displaying a heterogeneous pattern. In parallel, loss of βII spectrin results in reorganization of the microtubule network that may underlie the heterogeneous RyR_2 distribution. Alternatively, microtubule reorganization may be a compensatory response of the cell to βII spectrin loss because we also identified increased expression of βI spectrin (Figure XII in the online-only Data Supplement). Notably, abnormal organization of the calcium release structure was also identified in a mutant mouse model harboring a calsequestrin mutation linked to human catecholaminergic polymorphic ventricular tachycardia.[42] These mice, like the βII spectrin cKO mice, display unstable electric events and significant cytosolic calcium management phenotypes. Beyond spectrin, junctophilin, a lipophilic molecule anchored to the junctional SR, has also been linked to the organization of the ryanodine receptor in heart. In fact, *JPH2*$^{-/-}$ mice are embryonic lethal and display an enlarged dyadic cleft.[43] Although organization of RyR_2 is altered in βII spectrin cKO mice, we observed normal localization and expression of T-tubule L-type calcium channels ($Ca_v1.2$). Furthermore, we observed no difference in T-tubule morphology between control and βII spectrin cKO mice through Di-8-ANEPPS imaging. Therefore, the βII spectrin pathway appears to regulate select populations of membrane proteins without altering membrane morphology. It will be critical for future experiments to define the specific pathways underlying βII spectrin–dependent regulation of RyR_2 clusters. Importantly, βII spectrin–dependent regulation of RyR_2 clusters is likely independent of ankyrin-B because ankyrin-B$^{+/-}$ mice display no defects in RyR_2 expression or localization.[10] Finally, our work supports a relationship between βII spectrin and the microtubule system. Because spectrins have previously been linked to microtubule-based proteins, including kinesin II and the dynein complex,[44–46] and spectrin-associated proteins, including protein 4.1R, have been linked to arrhythmia in animals,[47] work to integrate the role of the βII spectrin pathway with intracellular targeting versus cytoskeletal organization will be an important future area of research. Likewise, because our data show accelerated heart failure phenotypes in βII spectrin cKO mice (Figure 8), it will be important to investigate the long-term function of βII spectrin in well-phenotyped human and animal disease models.

Sources of Funding

This work was supported by National Institutes of Health grants HL114893 (Dr Hund), HL084583, HL083422, and HL114383 (Dr Mohler); James S. McDonell Foundation (Dr Hund); American Heart Association (Dr Mohler); National Center for Advancing Translational Sciences TL1TR001069 (Dr Smith); Indiana University Health–Indiana University School of Medicine Strategic Research Initiative (Drs Spoonamore and Vatta); South University of Science and Technology of China (Dr Wei); and European–North American Atrial Fibrillation Research Alliance (07CVD03, Dr Dobrev) grant of Fondation Leducq.

Disclosures

None.

References

1. Moulik M, Vatta M, Witt SH, Arola AM, Murphy RT, McKenna WJ, Boriek AM, Oka K, Labeit S, Bowles NE, Arimura T, Kimura A, Towbin JA. ANKRD1, the gene encoding cardiac ankyrin repeat protein, is a novel dilated cardiomyopathy gene. *J Am Coll Cardiol*. 2009;54:325–333. doi: 10.1016/j.jacc.2009.02.076.
2. Lammerding J, Schulze PC, Takahashi T, Kozlov S, Sullivan T, Kamm RD, Stewart CL, Lee RT. Lamin A/C deficiency causes defective nuclear mechanics and mechanotransduction. *J Clin Invest*. 2004;113:370–378. doi: 10.1172/JCI19670.
3. van Tintelen JP, Entius MM, Bhuiyan ZA, Jongbloed R, Wiesfeld AC, Wilde AA, van der Smagt J, Boven LG, Mannens MM, van Langen IM, Hofstra RM, Otterspoor LC, Doevendans PA, Rodriguez LM, van Gelder IC, Hauer RN. Plakophilin-2 mutations are the major determinant of familial arrhythmogenic right ventricular dysplasia/cardiomyopathy. *Circulation*. 2006;113:1650–1658. doi: 10.1161/CIRCULATIONAHA.105.609719.
4. Stroud MJ, Banerjee I, Veevers J, Chen J. Linker of nucleoskeleton and cytoskeleton complex proteins in cardiac structure, function, and disease. *Circ Res*. 2014;114:538–548. doi: 10.1161/CIRCRESAHA.114.301236.
5. Schwartz PJ, Ackerman MJ, George AL Jr, Wilde AA. Impact of genetics on the clinical management of channelopathies. *J Am Coll Cardiol*. 2013;62:169–180. doi: 10.1016/j.jacc.2013.04.044.
6. Ackerman MJ, Mohler PJ. Defining a new paradigm for human arrhythmia syndromes: phenotypic manifestations of gene mutations in ion channel- and transporter-associated proteins. *Circ Res*. 2010;107:457–465. doi: 10.1161/CIRCRESAHA.110.224592.
7. Cunha SR, Hund TJ, Hashemi S, Voigt N, Li N, Wright P, Koval O, Li J, Gudmundsson H, Gumina RJ, Karck M, Schott JJ, Probst V, Le Marec H, Anderson ME, Dobrev D, Wehrens XH, Mohler PJ. Defects in ankyrin-based membrane protein targeting pathways underlie atrial fibrillation. *Circulation*. 2011;124:1212–1222. doi: 10.1161/CIRCULATIONAHA.111.023986.
8. Le Scouarnec S, Bhasin N, Vieyres C, Hund TJ, Cunha SR, Koval O, Marionneau C, Chen B, Wu Y, Demolombe S, Song LS, Le Marec H, Probst V, Schott JJ, Anderson ME, Mohler PJ. Dysfunction in ankyrin-B-dependent ion channel and transporter targeting causes human sinus node disease. *Proc Natl Acad Sci USA*. 2008;105:15617–15622. doi: 10.1073/pnas.0805500105.

9. Mohler PJ, Le Scouarnec S, Denjoy I, Lowe JS, Guicheney P, Caron L, Driskell IM, Schott JJ, Norris K, Leenhardt A, Kim RB, Escande D, Roden DM. Defining the cellular phenotype of "ankyrin-B syndrome" variants: human ANK2 variants associated with clinical phenotypes display a spectrum of activities in cardiomyocytes. *Circulation*. 2007;115:432–441. doi: 10.1161/CIRCULATIONAHA.106.656512.
10. Mohler PJ, Schott JJ, Gramolini AO, Dilly KW, Guatimosim S, duBell WH, Song LS, Haurogné K, Kyndt F, Ali ME, Rogers TB, Lederer WJ, Escande D, Le Marec H, Bennett V. Ankyrin-B mutation causes type 4 long-QT cardiac arrhythmia and sudden cardiac death. *Nature*. 2003;421:634–639. doi: 10.1038/nature01335.
11. Mohler PJ, Splawski I, Napolitano C, Bottelli G, Sharpe L, Timothy K, Priori SG, Keating MT, Bennett V. A cardiac arrhythmia syndrome caused by loss of ankyrin-B function. *Proc Natl Acad Sci USA*. 2004;101:9137–9142. doi: 10.1073/pnas.0402546101.
12. Ipsaro JJ, Mondragón A. Structural basis for spectrin recognition by ankyrin. *Blood*. 2010;115:4093–4101. doi: 10.1182/blood-2009-11-255604.
13. Mohler PJ, Yoon W, Bennett V. Ankyrin-B targets beta2-spectrin to an intracellular compartment in neonatal cardiomyocytes. *J Biol Chem*. 2004;279:40185–40193. doi: 10.1074/jbc.M406018200.
14. Wang C, Yu C, Ye F, Wei Z, Zhang M. Structure of the ZU5-ZU5-UPA-DD tandem of ankyrin-B reveals interaction surfaces necessary for ankyrin function. *Proc Natl Acad Sci USA*. 2012;109:4822–4827. doi: 10.1073/pnas.1200613109.
15. Pogwizd SM. Focal mechanisms underlying ventricular tachycardia during prolonged ischemic cardiomyopathy. *Circulation*. 1994;90:1441–1458.
16. Pogwizd SM, Qi M, Yuan W, Samarel AM, Bers DM. Upregulation of Na(+)/Ca(2+) exchanger expression and function in an arrhythmogenic rabbit model of heart failure. *Circ Res*. 1999;85:1009–1019.
17. Baddeley D, Jayasinghe ID, Lam L, Rossberger S, Cannell MB, Soeller C. Optical single-channel resolution imaging of the ryanodine receptor distribution in rat cardiac myocytes. *Proc Natl Acad Sci USA*. 2009;106:22275–22280. doi: 10.1073/pnas.0908971106.
18. Go LO, Moschella MC, Watras J, Handa KK, Fyfe BS, Marks AR. Differential regulation of two types of intracellular calcium release channels during end-stage heart failure. *J Clin Invest*. 1995;95:888–894. doi: 10.1172/JCI117739.
19. van Oort RJ, Garbino A, Wang W, Dixit SS, Landstrom AP, Gaur N, De Almeida AC, Skapura DG, Rudy Y, Burns AR, Ackerman MJ, Wehrens XH. Disrupted junctional membrane complexes and hyperactive ryanodine receptors after acute junctophilin knockdown in mice. *Circulation*. 2011;123:979–988. doi: 10.1161/CIRCULATIONAHA.110.006437.
20. Terentyev D, Nori A, Santoro M, Viatchenko-Karpinski S, Kubalova Z, Gyorke I, Terentyeva R, Vedamoorthyrao S, Blom NA, Valle G, Napolitano C, Williams SC, Volpe P, Priori SG, Gyorke S. Abnormal interactions of calsequestrin with the ryanodine receptor calcium release channel complex linked to exercise-induced sudden cardiac death. *Circ Res*. 2006;98:1151–1158. doi: 10.1161/01.RES.0000220647.93982.08.
21. Mohler PJ, Gramolini AO, Bennett V. The ankyrin-B C-terminal domain determines activity of ankyrin-B/G chimeras in rescue of abnormal inositol 1,4,5-trisphosphate and ryanodine receptor distribution in ankyrin-B (–/–) neonatal cardiomyocytes. *J Biol Chem*. 2002;277:10599–10607. doi: 10.1074/jbc.M110958200.
22. Makara MA, Curran J, Little SC, Musa H, Polina I, Smith SA, Wright PJ, Unudurthi SD, Snyder J, Bennett V, Hund TJ, Mohler PJ. Ankyrin-G coordinates intercalated disc signaling platform to regulate cardiac excitability in vivo. *Circ Res*. 2014;115:929–938. doi: 10.1161/CIRCRESAHA.115.305154.
23. DeGrande S, Nixon D, Koval O, Curran JW, Wright P, Wang Q, Kashef F, Chiang D, Li N, Wehrens XH, Anderson ME, Hund TJ, Mohler PJ. CaMKII inhibition rescues proarrhythmic phenotypes in the model of human ankyrin-B syndrome. *Heart Rhythm*. 2012;9:2034–2041. doi: 10.1016/j.hrthm.2012.08.026.
24. Blikstad I, Nelson WJ, Moon RT, Lazarides E. Synthesis and assembly of spectrin during avian erythropoiesis: stoichiometric assembly but unequal synthesis of alpha and beta spectrin. *Cell*. 1983;32:1081–1091.
25. Moon RT, Lazarides E. Biogenesis of the avian erythroid membrane skeleton: receptor-mediated assembly and stabilization of ankyrin (goblin) and spectrin. *J Cell Biol*. 1984;98:1899–1904.
26. Woods CM, Lazarides E. Degradation of unassembled alpha- and beta-spectrin by distinct intracellular pathways: regulation of spectrin topogenesis by beta-spectrin degradation. *Cell*. 1985;40:959–969.
27. Heling A, Zimmermann R, Kostin S, Maeno Y, Hein S, Devaux B, Bauer E, Klövekorn WP, Schlepper M, Schaper W, Schaper J. Increased expression of cytoskeletal, linkage, and extracellular proteins in failing human myocardium. *Circ Res*. 2000;86:846–853.
28. Agre P, Orringer EP, Bennett V. Deficient red-cell spectrin in severe, recessively inherited spherocytosis. *N Engl J Med*. 1982;306:1155–1161. doi: 10.1056/NEJM198205133061906.
29. Stankewich MC, Cianci CD, Stabach PR, Ji L, Nath A, Morrow JS. Cell organization, growth, and neural and cardiac development require αII-spectrin. *J Cell Sci*. 2011;124(pt 23):3956–3966. doi: 10.1242/jcs.080374.
30. Tang Y, Katuri V, Dillner A, Mishra B, Deng CX, Mishra L. Disruption of transforming growth factor-beta signaling in ELF beta-spectrin-deficient mice. *Science*. 2003;299:574–577. doi: 10.1126/science.1075994.
31. Kizhatil K, Bennett V. Lateral membrane biogenesis in human bronchial epithelial cells requires 190-kDa ankyrin-G. *J Biol Chem*. 2004;279:16706–16714. doi: 10.1074/jbc.M314296200.
32. Yang Y, Lacas-Gervais S, Morest DK, Solimena M, Rasband MN. BetaIV spectrins are essential for membrane stability and the molecular organization of nodes of Ranvier. *J Neurosci*. 2004;24:7230–7240. doi: 10.1523/JNEUROSCI.2125-04.2004.
33. Galiano MR, Jha S, Ho TS, Zhang C, Ogawa Y, Chang KJ, Stankewich MC, Mohler PJ, Rasband MN. A distal axonal cytoskeleton forms an intra-axonal boundary that controls axon initial segment assembly. *Cell*. 2012;149:1125–1139. doi: 10.1016/j.cell.2012.03.039.
34. Zhang C, Susuki K, Zollinger DR, Dupree JL, Rasband MN. Membrane domain organization of myelinated axons requires βII spectrin. *J Cell Biol*. 2013;203:437–443. doi: 10.1083/jcb.201308116.
35. Armbrust KR, Wang X, Hathorn TJ, Cramer SW, Chen G, Zu T, Kangas T, Zink AN, Öz G, Ebner TJ, Ranum LP. Mutant β-III spectrin causes mGluR1α mislocalization and functional deficits in a mouse model of spinocerebellar ataxia type 5. *J Neurosci*. 2014;34:9891–9904. doi: 10.1523/JNEUROSCI.0876-14.2014.
36. Stankewich MC, Gwynn B, Ardito T, Ji L, Kim J, Robledo RF, Lux SE, Peters LL, Morrow JS. Targeted deletion of betaIII spectrin impairs synaptogenesis and generates ataxic and seizure phenotypes. *Proc Natl Acad Sci USA*. 2010;107:6022–6027. doi: 10.1073/pnas.1001522107.
37. Holleran EA, Ligon LA, Tokito M, Stankewich MC, Morrow JS, Holzbaur EL. Beta III spectrin binds to the Arp1 subunit of dynactin. *J Biol Chem*. 2001;276:36598–36605. doi: 10.1074/jbc.M104838200.
38. Ikeda Y, Dick KA, Weatherspoon MR, Gincel D, Armbrust KR, Dalton JC, Stevanin G, Dürr A, Zühlke C, Bürk K, Clark HB, Brice A, Rothstein JD, Schut LJ, Day JW, Ranum LP. Spectrin mutations cause spinocerebellar ataxia type 5. *Nat Genet*. 2006;38:184–190. doi: 10.1038/ng1728.
39. Shan J, Kushnir A, Betzenhauser MJ, Reiken S, Li J, Lehnart SE, Lindegger N, Mongillo M, Mohler PJ, Marks AR. Phosphorylation of the ryanodine receptor mediates the cardiac fight or flight response in mice. *J Clin Invest*. 2010;120:4388–4398. doi: 10.1172/JCI32726.
40. van Oort RJ, McCauley MD, Dixit SS, Pereira L, Yang Y, Respress JL, Wang Q, De Almeida AC, Skapura DG, Anderson ME, Bers DM, Wehrens XH. Ryanodine receptor phosphorylation by calcium/calmodulin-dependent protein kinase II promotes life-threatening ventricular arrhythmias in mice with heart failure. *Circulation*. 2010;122:2669–2679. doi: 10.1161/CIRCULATIONAHA.110.982298.
41. Kannankeril PJ, Mitchell BM, Goonasekera SA, Chelu MG, Zhang W, Sood S, Kearney DL, Danila CI, De Biasi M, Wehrens XH, Pautler RG, Roden DM, Taffet GE, Dirksen RT, Anderson ME, Hamilton SL. Mice with the R176Q cardiac ryanodine receptor mutation exhibit catecholamine-induced ventricular tachycardia and cardiomyopathy. *Proc Natl Acad Sci USA*. 2006;103:12179–12184. doi: 10.1073/pnas.0600268103.
42. Liu N, Denegri M, Dun W, Boncompagni S, Lodola F, Protasi F, Napolitano C, Boyden PA, Priori SG. Abnormal propagation of calcium waves and ultrastructural remodeling in recessive catecholaminergic polymorphic ventricular tachycardia. *Circ Res*. 2013;113:142–152. doi: 10.1161/CIRCRESAHA.113.301783.
43. Takeshima H, Komazaki S, Nishi M, Iino M, Kangawa K. Junctophilins: a novel family of junctional membrane complex proteins. *Mol Cell*. 2000;6:11–22.
44. Papal S, Cortese M, Legendre K, Sorusch N, Dragavon J, Sahly I, Shorte S, Wolfrum U, Petit C, El-Amraoui A. The giant spectrin βV couples the molecular motors to phototransduction and Usher syndrome type I

proteins along their trafficking route. *Hum Mol Genet*. 2013;22:3773–3788. doi: 10.1093/hmg/ddt228.
45. Ayalon G, Davis JQ, Scotland PB, Bennett V. An ankyrin-based mechanism for functional organization of dystrophin and dystroglycan. *Cell*. 2008;135:1189–1200. doi: 10.1016/j.cell.2008.10.018.
46. Pielage J, Cheng L, Fetter RD, Carlton PM, Sedat JW, Davis GW. A presynaptic giant ankyrin stabilizes the NMJ through regulation of presynaptic microtubules and transsynaptic cell adhesion. *Neuron*. 2008;58:195–209. doi: 10.1016/j.neuron.2008.02.017.
47. Stagg MA, Carter E, Sohrabi N, Siedlecka U, Soppa GK, Mead F, Mohandas N, Taylor-Harris P, Baines A, Bennett P, Yacoub MH, Pinder JC, Terracciano CM. Cytoskeletal protein 4.1R affects repolarization and regulates calcium handling in the heart. *Circ Res*. 2008;103:855–863. doi: 10.1161/CIRCRESAHA.108.176461.

CLINICAL PERSPECTIVE

Cardiovascular disease remains the number one cause of death in the United States and is a major and growing public health problem worldwide. Each year, ≈785 000 Americans experience a heart attack, and these events significantly increase the risk for deadly ventricular arrhythmias after myocardial infarction. Despite the fact that cardiac arrhythmias lead to >300 000 deaths per year, current arrhythmia therapies targeting ion channels unfortunately either are suboptimal or lead to increased mortality. The cardiac cytoskeleton is a highly ordered array of structural, regulatory, and accessory proteins spanning from the plasma membrane to the nucleus. This evolved network has emerged as a central governing factor in the control of cardiac membrane integrity, and dysfunction in cytoskeleton and cytoskeleton-associated proteins is now directly linked to cardiac myopathies and dystrophies. However, the role of the cytoskeleton in normal cardiac electric function is not well resolved. On the basis of clinical and genetic findings from a proband with severe ventricular arrhythmia and cardiac arrest, we identified βII spectrin as critical for the organization of myocyte membrane and membrane-associated proteins. Dysfunction in this pathway in mice results in severe arrhythmia phenotypes associated with aberrant calcium. These findings provide a new mechanism for human arrhythmia and identify unexpected new roles for the cardiac cytoskeleton in human cardiovascular disease. Furthermore, these new data provide new insight into the complex mechanisms governing cardiac myocyte physiology.

Dysfunction in the βII Spectrin–Dependent Cytoskeleton Underlies Human Arrhythmia

Sakima A. Smith, Amy C. Sturm, Jerry Curran, Crystal F. Kline, Sean C. Little, Ingrid M. Bonilla, Victor P. Long, Michael Makara, Iuliia Polina, Langston D. Hughes, Tyler R. Webb, Zhiyi Wei, Patrick Wright, Niels Voigt, Deepak Bhakta, Katherine G. Spoonamore, Chuansheng Zhang, Raul Weiss, Philip F. Binkley, Paul M. Janssen, Ahmet Kilic, Robert S. Higgins, Mingzhai Sun, Jianjie Ma, Dobromir Dobrev, Mingjie Zhang, Cynthia A. Carnes, Matteo Vatta, Matthew N. Rasband, Thomas J. Hund and Peter J. Mohler

Circulation. 2015;131:695-708; originally published online January 28, 2015;
doi: 10.1161/CIRCULATIONAHA.114.013708
Circulation is published by the American Heart Association, 7272 Greenville Avenue, Dallas, TX 75231

Print ISSN: 0009-7322. Online ISSN: 1524-4539

SUPPLEMENTAL MATERIAL

Supplemental Methods

Ankyrin-B βII spectrin conditional knock-out (cKO) mice. Ankyrin-B cKO mice were generated by the introduction of LoxP sites flanking exon 24 of *Ank2*. The strategy results in the deletion of 73 bp of coding sequence: the splicing of exon 23-exon 25 leads to a frame shift resulting in a premature stop codon in exon 25. Mice were crossed to generate pure lines of floxed mice devoid of the neomycin cassette. Mice were screened by PCR and Southern analyses (genOway). Animals were crossed with mice expressing Cre under the cardiac promoter α-myosin heavy chain (αMHC-Cre) resulting in specific loss of ankyrin-B in adult cardiac myocytes. βII spectrin cKO mice were generated by the introduction of LoxP sites flanking exon 3 of the gene.[1] These animals were then crossed with αMHC-Cre mice.

Immunoblots and immunostaining. Tissue was harvested and immediately placed into ice cold homogenization buffer (in mM: 50 Tris-HCl, 10 NaCl, 320 sucrose, 5 EDTA, 2.5 EGTA; supplemented with 1:1000 protease inhibitor cocktail and 1:1000 PMSF). Following quantification, tissue lysates were analyzed on Mini-PROTEAN tetra cell (BioRad) on a 4-15% precast TGX gel (BioRad). Gels were transferred to a nitrocellulose membrane using the Mini-PROTEAN tetra cell (BioRad). Membranes were blocked for 1 hour at room temperature using a 3% BSA solution or 5% milk solution and incubated with primary antibody overnight at 4°C. Densitometry analysis was done using ImageLab software (BioRad). For all experiments, protein values were normalized against an internal loading control (actin, GAPDH, calsequestrin).

Super-resolution image acquisition, reconstruction, and sample preparation. Our custom built STORM system is based on an inverted microscope (IX71, Olympus America Inc.) with 1.49 NA 100x oil

immersion total internal reflection fluorescence (TIRF) objective. A 647 nm diode laser (Vortran Laser Technology Inc.) is used to both excite and activate Alexa Fluor 647 (Life Technologies, CA). An EMCCD camera (iXon Ultra 897, Andor Technologies, CT) is used for image acquisition. The sample holder is mounted on a 3D piezo stage (Nano- LPS, Mad City Lab). An infrared 980 nm laser is used in combination with the piezo stage for the axial Zero Drift Correction (ZDC).[2] The super-resolution image is reconstructed using a tracklet-based method as described.[3] The effective resolution is approximately 35 nm. Control or βII spectrin cKO cardiomyocytes were labeled using RyR_2 or βII-spectrin primary antibody as described [4] for 24 hours. Cells were then washed and incubated with an Alexa Fluor 647 conjugated secondary goat-anti-mouse (Life Technologies, CA) or goat-anti-rabbit secondary antibody (Life Technologies, CA) for 3 hours at room temperature. Glass bottom culture dishes (MatTek, MA) were coated with Matrigel (Corning Inc, MA, 1:6 dilution) for 45 minutes. 50 μl labeled cell suspension was pipetted into the dish and settled for 1 hour before washing with the imaging buffer.[5] Cells were imaged in the imaging buffer and typically 60,000 to 80,000 frames were acquired with a frame rate of 56 fps.

Site Directed Mutagenesis. Primers were designed to insert the p.R990Q mutations into the spectrin-binding domain of ankyrin-B in pcDNA3.1+. Primers were used in concert with the Stratagene QuikChange Site-Direct Mutagenesis kit and manufacturer's instructions. Sequences were verified before experiments.

Production and purification of fusion proteins. cDNAs for the WT ankyrin-B, and p.R990Q spectrin-binding domains were PCR-amplified, cloned into pGEX6P-1 (Amersham), and sequenced to confirm correct sequences. To facilitate cloning, all constructs were engineered to contain 5′ *Eco*RI and 3′ *Xho*I restriction sites. BL21(DE3)pLysS cells were transformed with the ankyrin-B pGEX6P-1 constructs and grown overnight at 37 °C in LB supplemented with 0.05 g/L ampicillin. The overnight cultures were

subcultured for large-scale expression. Cells were grown to an optical density of 0.6 and induced with 1 mM isopropyl 1-thio-α-D-galactopyranoside (IPTG) for 4 h at 37 °C. Cells were centrifuged for 10 min at 8,000 x *g*, re-suspended in PBS, and frozen at -80 °C following re-suspension. Cells were lysed by thawing. The crude extract was suspended in a solution of PBS, 1 mM DTT, 1 mM EDTA, 40 g/mL AEBSF, 10 g/mL leupeptin, 40 g/mL benzamidine, 10 g/mL peptstatin (Lysis buffer). Lysates were homogenized by sonication, centrifuged to remove cellular debris, and the supernatant incubated with glutathione-sepharose overnight at 4 °C. The overnight incubation was centrifuged and washed in PBS. A small aliquot was separated by SDS-PAGE and Coomassie Blue stained to quantitate immobilized protein.

ECG experiments. ECG recordings of ambulatory mice were obtained using subcutaneously implanted radiotelemeters (DSI, St. Paul, MN). For baseline HR analysis, continuous ECG data was collected for 1 hour on seven separate days. Only ECG complexes with clearly defined onset and termination signals were sampled. ECG parameter measurement was performed by one individual and confirmed by two or more individuals. For stress tests, mice were initially injected intraperitoneally with both low dose (0.2 mg/kg) and high dose (2 mg/kg) epinephrine. Baseline recordings were performed prior to each injection for at least 5 minutes and for at least 15 minutes after the injection. Non-sustained and sustained arrhythmias were identified using standard ECG analysis guidelines. Variability was assessed over a 10 min period and expressed as the average heart rate plus standard deviation. In a separate group of mice, surface ECG recordings were obtained under anesthesia with 2% isoflurane. Three needle electrodes were placed subcutaneously in the standard limb configuration. For each mouse, 15 min of continuous data were sampled at 4 kHz with a PowerLab 4/30 interface (AD Instruments). Analysis was performed offline using LabChart 7 Pro (AD Instruments).

Electrophysiology. Membrane currents were assessed by use of an Axopatch-200B amplifier and a CV-203BU head stage (Axon Instruments). Experimental control, data acquisition, and data analysis were accomplished with the use of software package PClamp 10 with the Digidata 1440A acquisition system (Axon Instruments).

Calcium wave studies. Isolated and fluo-4 loaded ventricular myocytes were analyzed for calcium waves. Myocytes were field stimulated at 0.5 Hz and upon cessation of stimulation were continuously monitored for spontaneous calcium wave formation for 30 seconds. Data in Fig. 5K represents total spontaneous waves for each genotype over the 30 second interval. Fig. 5L represents waves/myocyte over the first 15 seconds of observation.

Action Potentials. Action potentials (APs) were performed using multiple pacing frequencies ± superfusion with 1μM isoproterenol. In parallel experiments, myocytes were pre-treated with 100 nM ryanodine.

Antibodies. The following antibodies were used in this study: mouse monoclonal anti-NCX1 (Swant), rabbit polyclonal anti-βII spectrin, ankyrin-B, ankyrin-R, and ankyrin-G, CaMKIIδ/CaMKIIδ pS287 (Badrilla), mouse monoclonal anti-$Ca_v1.2$ (Affinity Bioreagents), βI spectrin (neuromab), rabbit polyclonal anti-$Na_v1.5$[4], Na/K ATPase (Millipore), actin (Santa Cruz Biotechnology), α-actinin (Sigma), αII spectrin (Sigma), βII spectrin, connexin43 (Invitrogen), α-tubulin (Sigma), N-cadherin (Invitrogen), desmin (Sigma), GAPDH (Fitzgerald), RyR_2 and SERCA2 (Affinity Bioreagents).

Human variant rescue studies. Assays to evaluate human ankyrin-B mutations were performed in primary control and ankyrin-B cKO myocytes. Ankyrin-B R990Q, as well as two ankyrin-B mutations previously shown to lack βII spectrin-binding[6] (DAR976AAA, A1000P) were evaluated in parallel experiments.

In vitro binding assays. In vitro binding assays were performed as previously described using GST-fusion proteins and ^{35}S-labelled *in vitro* translation products. Reactions were performed at 4°C for 3 hours in a high stringency binding buffer (50 mM Tris pH 7.4, 1 mM EDTA, 1 mM EGTA, 500 mM NaCl, 0.1% Triton X-100), washed 5 times in a high stringency wash buffer (1 M NaCl binding buffer), separated by SDS-PAGE, and visualized by phosphorimaging. All binding experiments were replicated at least three times.

Structural modeling. Analysis of ankyrin-B/βII spectrin interactions were performed using the high resolution structure of the ankyrin-B ZZUD tandem. All structural figures were prepared using PyMOL (www.pymol.org).

Echocardiography. Transthoracic echocardiogram was performed using the Vevo 2100 (Visualsonics). The mice were anesthetized using 2.0 % isoflurane in 95% O2 / 5% CO_2 at a rate of ~ 0.8 L/min. Anesthesia was maintained by administration of oxygen and ~1% isoflurane. Electrode gel was placed on the ECG sensors of the heated platform and the mouse was placed supine on the platform to monitor electrical activity of heart. A temperature probe was inserted into the rectum of the mouse to monitor core temperature of ~ 37°C. The MS-400 transducer was used to collect the contractile parameters of the heart in the short axis M-mode. Transverse aortic constriction was performed as described.[7]

Neonatal cardiomyocyte experiments. Experiments were performed as described, however for transfections, unlike previous studies in global ankyrin-B$^{-/-}$ myocytes in post-natal day 1 myocytes[6] (done at P1 as global ankyrin-B mice die immediately after birth[8]), experiments in this manuscript were performed to evaluate expression in post-natal 7 day myocytes to coincide with expression and striation of βII spectrin in the myocyte. Based on our new findings, while βII spectrin requires ankyrin-B

expression in immature myocytes (<post-natal day 3), this relationship reverses by post-natal day 7 where βII spectrin expression is required for ankyrin-B expression.

References

1. Galiano MR, Jha S, Ho TS, Zhang C, Ogawa Y, Chang KJ, Stankewich MC, Mohler PJ, Rasband MN. A distal axonal cytoskeleton forms an intra-axonal boundary that controls axon initial segment assembly. *Cell*. 2012;149:1125-1139
2. Huang B, Wang W, Bates M, Zhuang X. Three-dimensional super-resolution imaging by stochastic optical reconstruction microscopy. *Science*. 2008;319:810-813
3. Sun M, Huang J, Bunyak F, Gumpper K, De G, Sermersheim M, Liu G, Lin PH, Palaniappan K, Ma J. Superresolution microscope image reconstruction by spatiotemporal object decomposition and association: Application in resolving t-tubule structure in skeletal muscle. *Opt Express*. 2014;22:12160-12176
4. Hund TJ, Koval OM, Li J, Wright PJ, Qian L, Snyder JS, Gudmundsson H, Kline CF, Davidson NP, Cardona N, Rasband MN, Anderson ME, Mohler PJ. A beta(iv)-spectrin/camkii signaling complex is essential for membrane excitability in mice. *J Clin Invest*. 2010;120:3508-3519
5. van de Linde S, Kasper R, Heilemann M, Sauer M. Photoswitching microscopy with standard fluorophores. *Applied Physics B*. 2008;93
6. Mohler PJ, Yoon W, Bennett V. Ankyrin-b targets beta2-spectrin to an intracellular compartment in neonatal cardiomyocytes. *J Biol Chem*. 2004;279:40185-40193
7. Gudmundsson H, Curran J, Kashef F, Snyder JS, Smith SA, Vargas-Pinto P, Bonilla IM, Weiss RM, Anderson ME, Binkley P, Felder RB, Carnes CA, Band H, Hund TJ, Mohler PJ. Differential regulation of ehd3 in human and mammalian heart failure. *J Mol Cell Cardiol*. 2012;52:1183-1190
8. Scotland P, Zhou D, Benveniste H, Bennett V. Nervous system defects of ankyrinb (-/-) mice suggest functional overlap between the cell adhesion molecule l1 and 440-kd ankyrinb in premyelinated axons. *J Cell Biol*. 1998;143:1305-1315.

Supplemental Figure 1

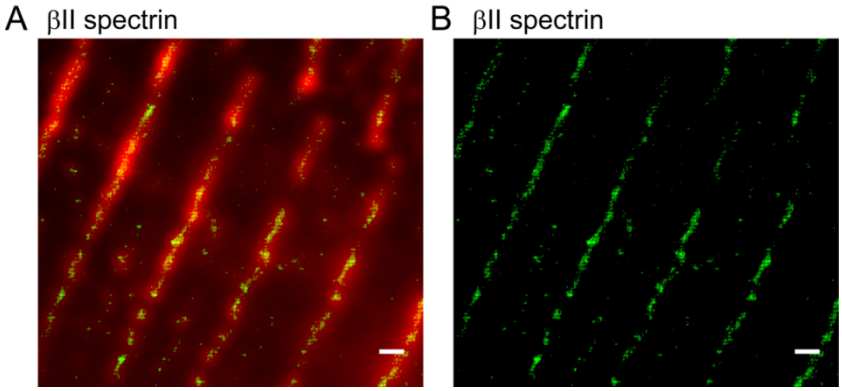

Supplemental Figure 1. Localization of βII spectrin in myocytes. (**A**) Overlay of a TIRF image (red) and the super-resolution image (green) of βII spectrin in control myocytes. (B) Super-resolution image of βII spectrin. Scale bar: 500 nm.

Supplemental Figure 2

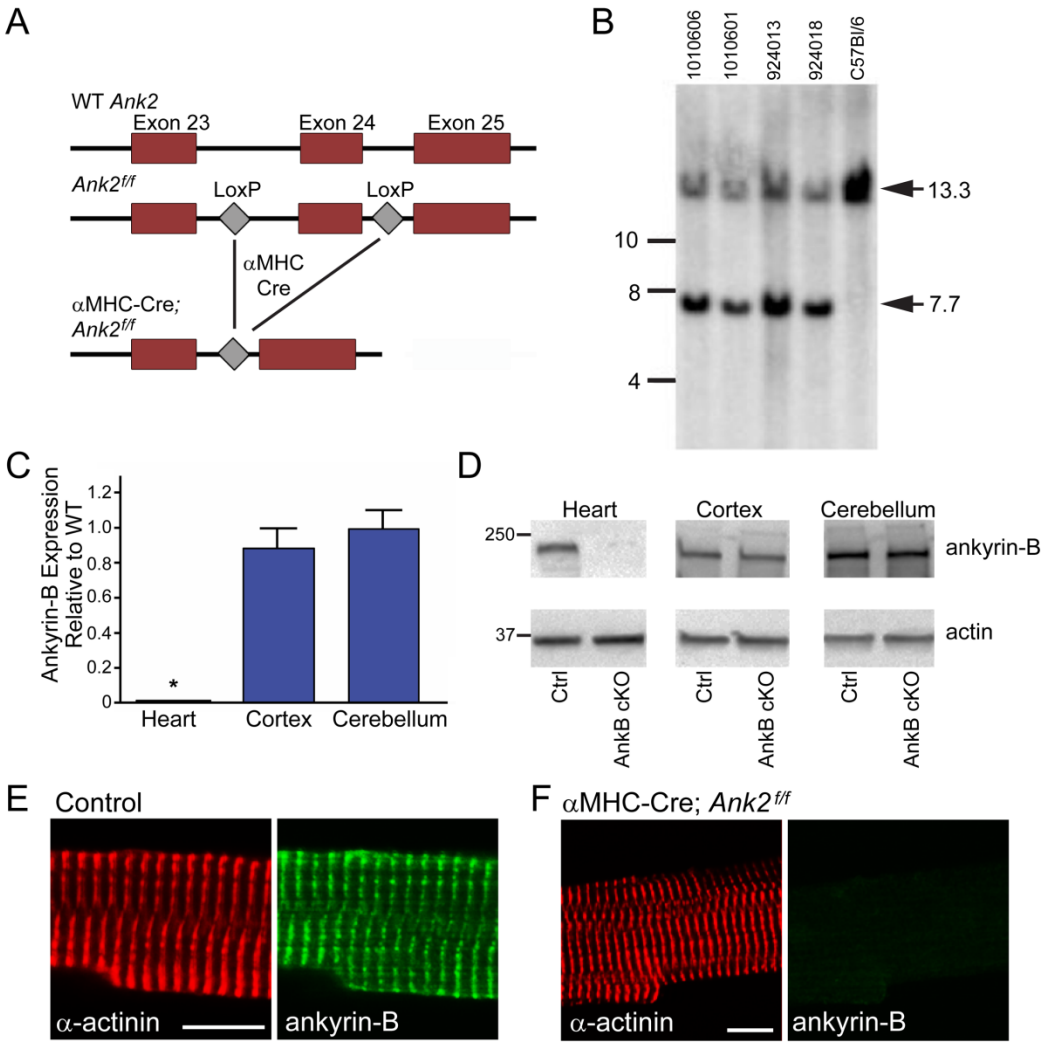

Supplemental Figure 2. Generation and validation of mice lacking ankyrin-B in ventricular cardiomyocytes. (**A**) Targeting strategy to generate Cre-dependent loss of cardiac ankyrin-B. (**B**) Southern blot analysis of heterozygous Neo-excised conditional knockout (αMHC-Cre; *Ank2*$^{f/f}$, cKO). Genomic DNA of tested animals was compared with WT DNA from C57/Bl6 mouse. Spe I digested DNAs were blotted on nylon membrane and hybridized with external 3' probe. (**C-D**) Expression of ankyrin-B in tissues from ankyrin-B cKO mouse relative to control mice ($p<0.05$ for ankyrin-B cKO heart compared with control heart). (**E-F**) Ankyrin-B immunostaining in control and ankyrin-B cKO mouse myocytes. Bar= 10 μm.

Supplemental Figure 3

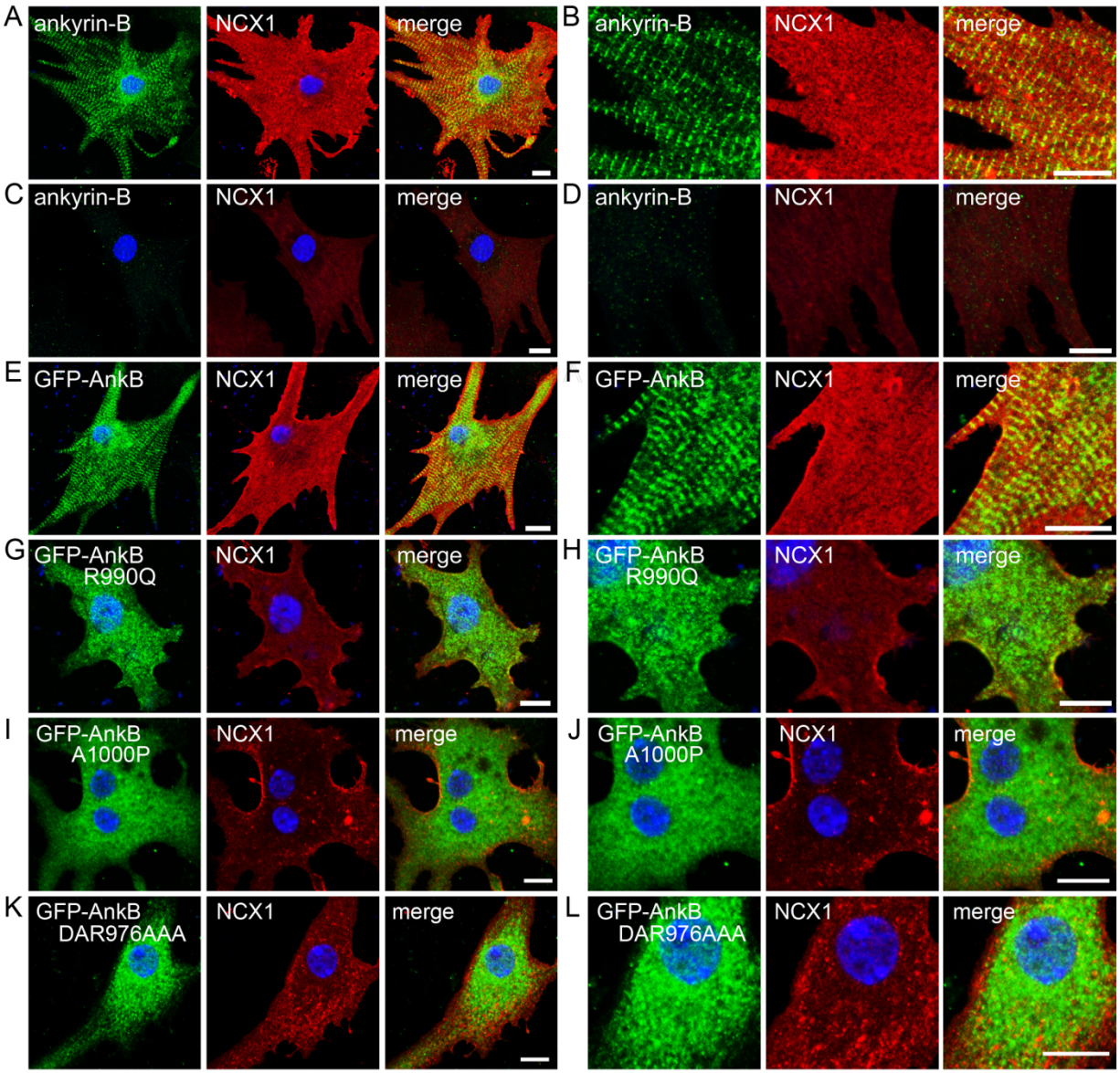

Supplemental Figure 3. Ankyrin-B R990Q in primary cardiomyocytes. Compared with control myocytes (**A-B**), ankyrin-B cKO myocytes (**C-D**) at post-natal day 7 display loss of ankyrin-B expression and membrane targeting of the Na/Ca exchanger (NCX1). (**E-F**) Expression of GFP-ankyrin-B is sufficient to rescue the striated pattern of ankyrin-B and NCX1 expression in ankyrin-B cKO myocytes. (**G-H**) While expressed in ankyrin-B cKO myocytes (green), GFP-ankyrin-B p.R990Q is abnormally localized and lacks ability to rescue abnormal Na/Ca exchanger localization. As a control for ankyrin-B R990Q, two mutant ankyrin-B polypeptides that lack βII spectrin-binding activity (**I-L**; A1000P, DAR976AAA) were analysed in parallel. Bar=10 μm.

Supplemental Figure 4

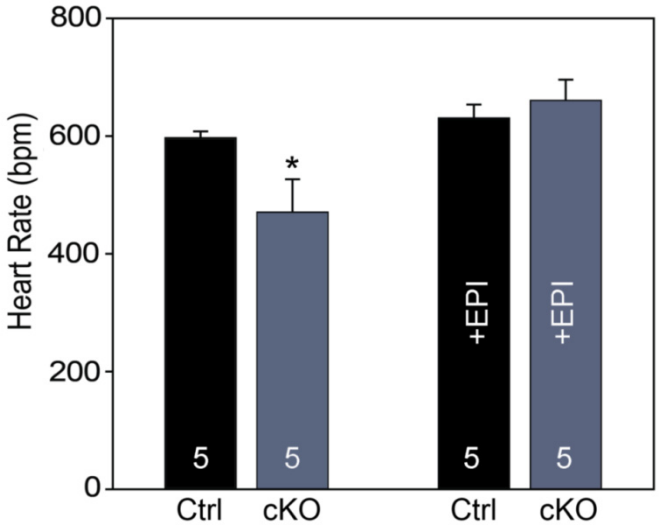

Supplemental Figure 4. βII spectrin cKO mice display bradycardia but normal peak heart rate response. Heart rate of conscious control mouse and βII spectrin cKO mice at baseline and following 2 mg/kg epinephrine I.P. Data represent mean heart rates of five mice/genotype recorded by telemetry ($p<0.05$ for cKO mice versus control mice at baseline).

Supplemental Figure 5

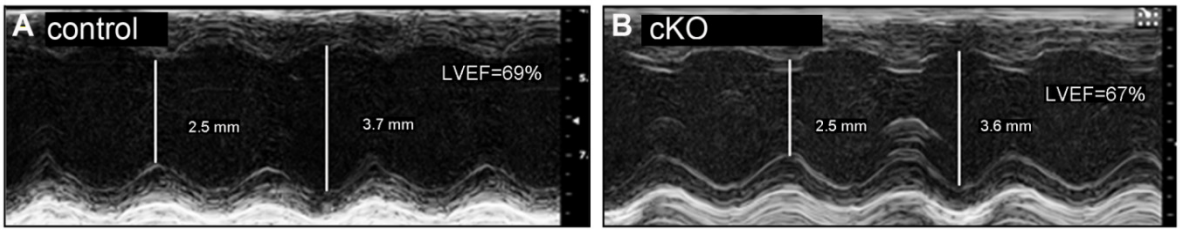

Supplemental Figure 5. βII spectrin cKO mice display normal cardiac function. (**A**) Normal baseline LVEF (69%) for 8 week old control mouse using M-mode end-systolic and -diastolic measurements. (**B**) Eight week βII spectrin cKO mouse with baseline LVEF of 67%.

Supplemental Figure 6

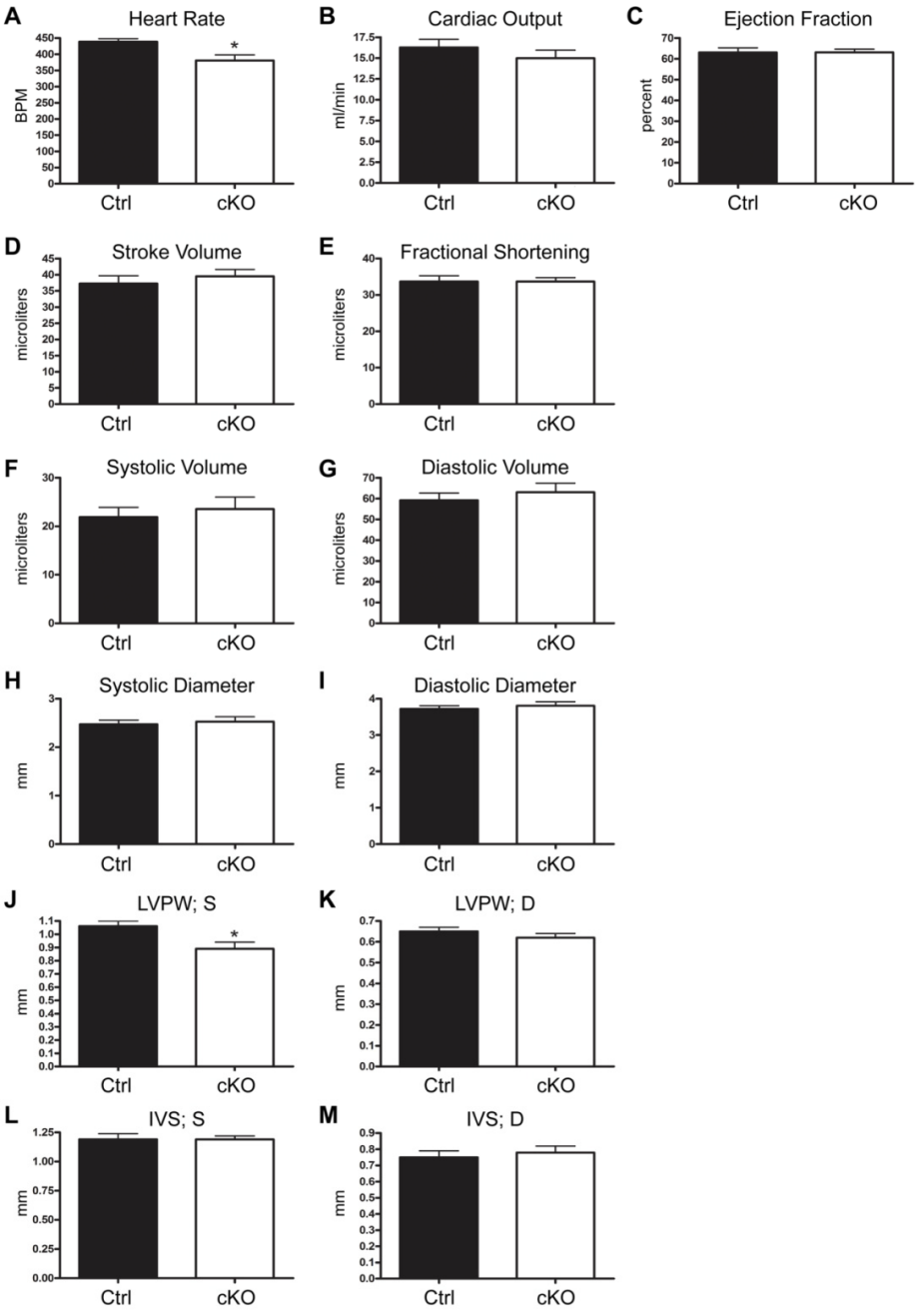

Supplemental Figure 6. βII spectrin cKO mouse cardiac measurements. (**A**) βII spectrin cKO mice displayed decreased heart rates when compared to control mice (n=5/genotype; $p<0.05$). There was no significant difference between control and βII spectrin cKO mice with respect to (**B**) cardiac output, (**C**) ejection fraction, (**D**) stoke volume, (**F**) systolic volume, (**G**) diastolic volume, (**E**) fractional shortening and (**H**) systolic and (**I**) diastolic diameter (n=5/genotype; N.S.). (**J**) Control mice displayed significantly more left ventricular posterior wall thickness (LVPW) during systole than βII spectrin cKO mice (n=5 mice/genotype, $p<0.05$). (**K**) LVPW thickness during diastole was similar between control and βII spectrin cKO mice (n=5 mice/genotype; N.S.). Intraventricular septal (IVS) thickness did not differ between control and βII spectrin cKO mice during systole (**L**) or diastole (**M**); (n=5 mice/genotype; N.S.).

Supplemental Figure 7

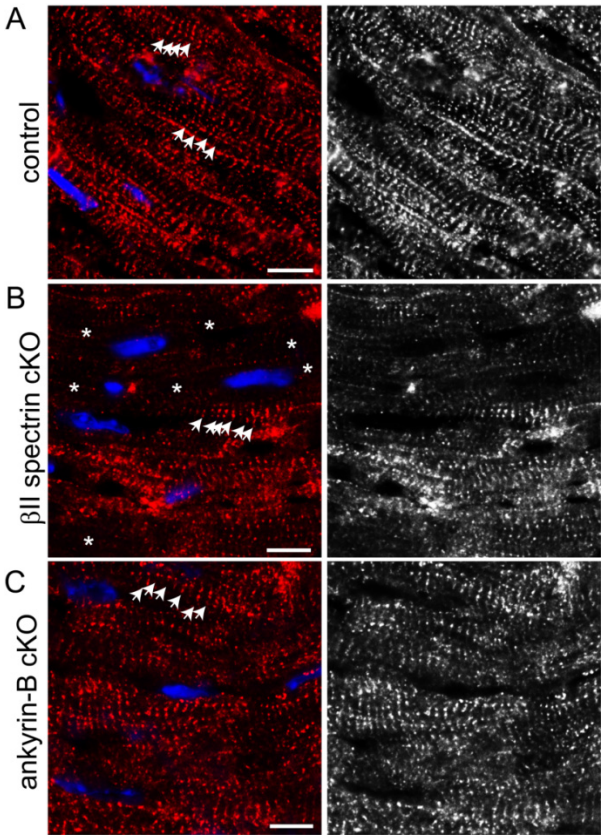

Supplemental Figure 7. βII spectrin cKO hearts display heterogeneity in RyR2 expression. RyR2 expression in (**A**) control, (**B**) βII spectrin cKO, and (**C**) ankyrin-B cKO left ventricle heart sections (multiple sections from n=3 hearts/genotype examined). RyR2 localization was generally homogeneous along the Z-line of control and ankyrin-B cKO hearts (white arrowheads), we observed heterogeneity in RyR2 expression both across myocyte sections as well as within single βII spectrin cKO myocytes (note * in panel B). Bar=10 μM.

Supplemental Figure 8

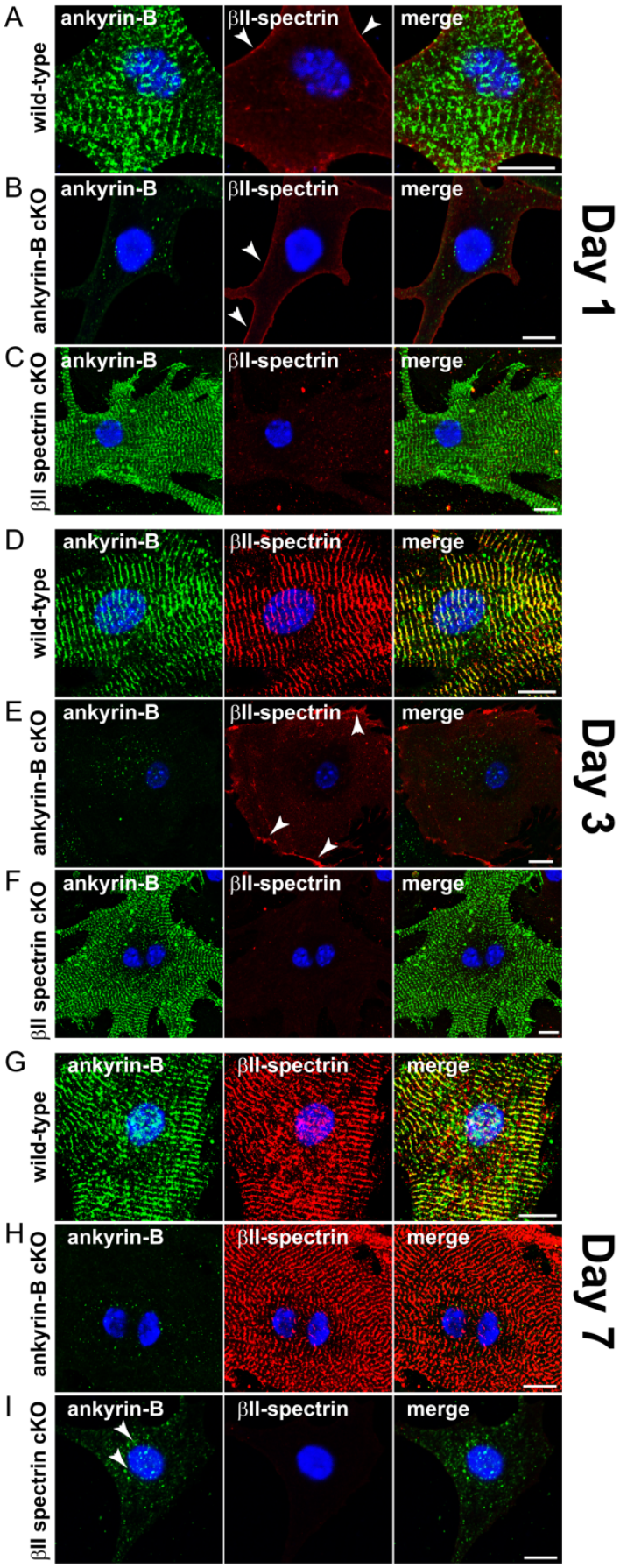

Supplemental Figure 8. Ankyrin-B targets βII spectrin in immature neonatal myocytes, whereas βII spectrin targets ankyrin-B in mature and adult myocytes. (**A-C**) Localization of ankyrin-B and βII spectrin in post-natal day 1 (P1) neonatal cardiomyocytes from control (**A**), ankyrin-B cKO (**B**), and βII spectrin cKO myocytes (**C**). Note that βII spectrin expression is minimal in the P1 myocyte whereas ankyrin-B is expressed and striated in control myocytes. Also note that ankyrin-B is expressed and striated in βII spectrin cKO myocytes. (**D-F**) At P3, βII spectrin is expressed in control myocytes and requires ankyrin-B for expression and localization. (**G-I**) In contrast to post-natal days 1-3, ankyrin-B is not required for βII spectrin expression or targeting. In fact, in these maturing myocytes, similar to adult myocytes, βII spectrin is required for ankyrin-B expression. Scale equals 10 microns in all panels.

Supplemental Figure 9

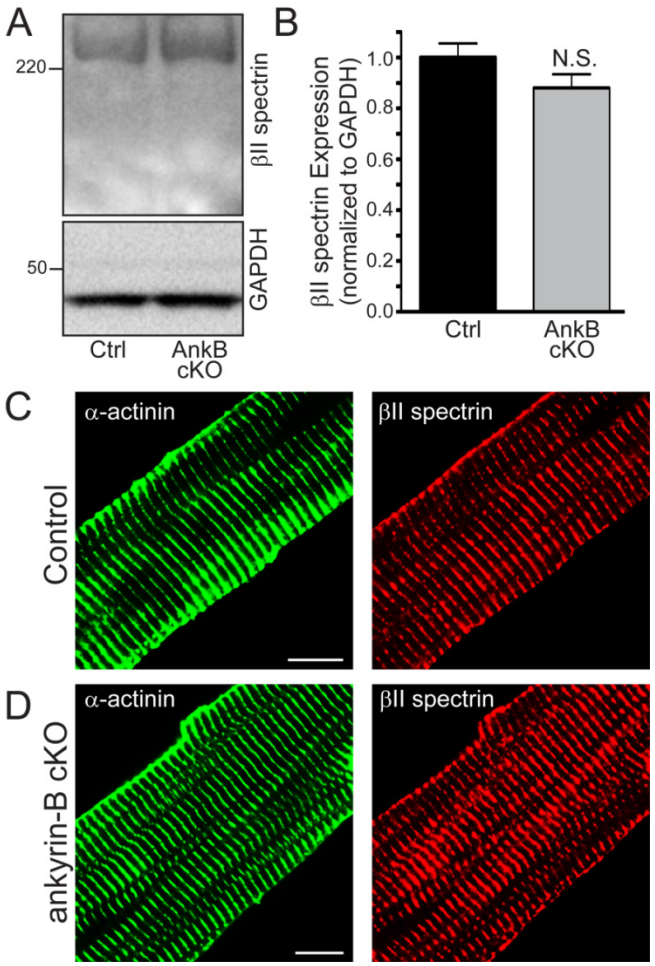

Supplemental Figure 9. βII spectrin levels are unchanged in hearts of ankyrin-B cKO mice. Expression levels of βII spectrin is not significantly different in protein lysates (A-B) from control (Ctrl, n=4) versus ankyrin-B cKO hearts (n=4; p=N.S.) or by immunostaining (C-D) of adult cardiomyocytes (red). Scale bar equals ten microns.

Supplemental Figure 10

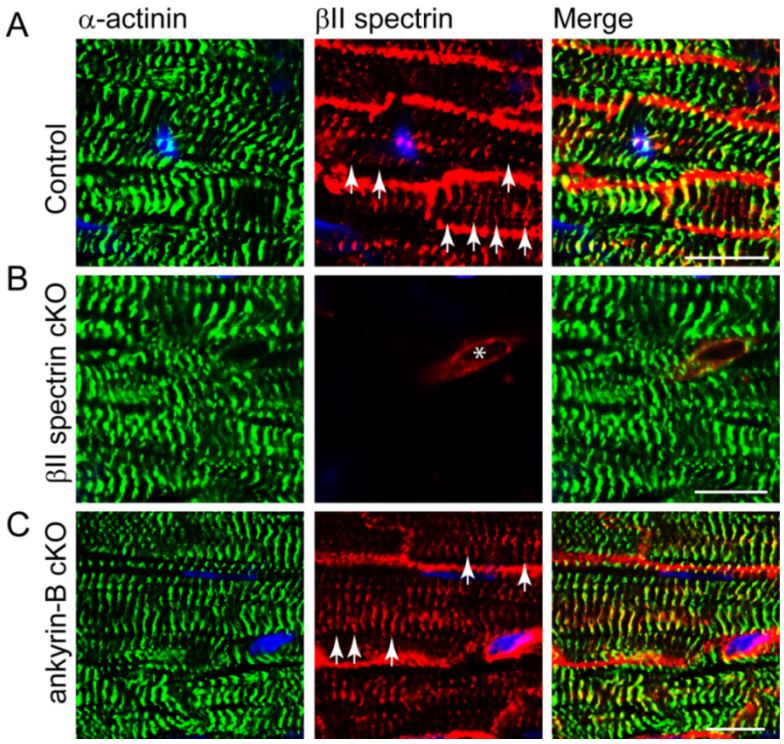

Supplemental Figure 10. Ankyrin-B is not required for βII spectrin expression or localization. βII spectrin localization (red) in control, βII spectrin cKO, and ankyrin-B cKO left ventricle. Sections are co-labeled with α-actinin. Note that in C, βII spectrin is normally expressed and striated in the absence of ankyrin-B. Also note that minor background of βII spectrin staining in βII spectrin cKO is small vessel (*), not ventricular myocytes. Bar=10 μM.

Supplemental Figure 11

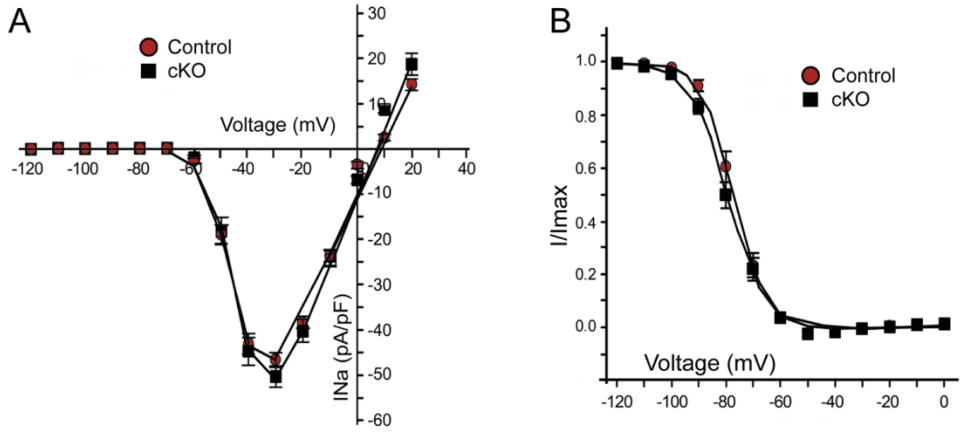

Supplemental Figure 11. βII spectrin deficiency does not alter cardiomyocyte INa. **(A-B)** Control (n=10) and βII spectrin cKO mouse myocytes (n=11) display no difference in I_{Na} phenotypes (N.S.).

Supplemental Figure 12

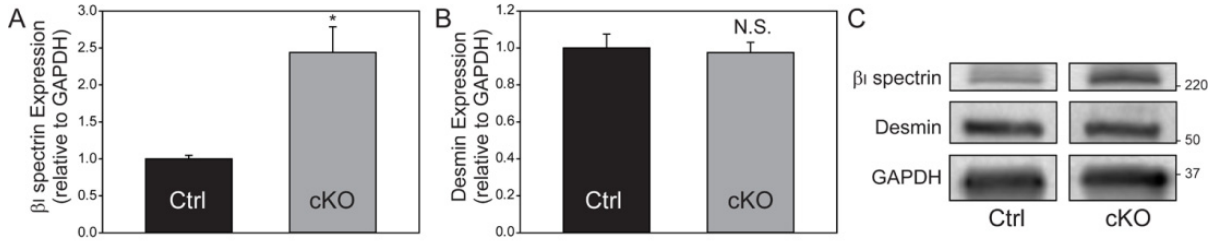

Supplemental Figure 12. βII spectrin deficiency results in increased expression of βI spectrin. **(A, C)** βI spectrin levels are increased nearly two-fold in βII spectrin cKO hearts (n=5) compared to control hearts (n=5 hearts; $p<0.05$). **(B,C)** Desmin expression levels are equivalent between control (n=5) and βII spectrin cKO hearts (n=5; p=N.S.).